HHS Public Access

Author manuscript

Curr Top Med Chem. Author manuscript; available in PMC 2018 March 04.

Published in final edited form as:

Curr Top Med Chem. 2017 ; 17(32): 3425–3443. doi:10.2174/1568026618666180118154514.

Conjugates of Cell Adhesion Peptides for Therapeutics and Diagnostics Against Cancer and Autoimmune Diseases

Mario E.G. Moral and **Teruna J. Siahaan**

Department of Pharmaceutical Chemistry, The University of Kansas, Simons Laboratory, 2095 Constant Ave., Lawrence, Kansas 66047, USA

Abstract

Overexpressed cell-surface receptors are hallmarks of many disease states and are often used as markers for targeting diseased cells over healthy counterparts. Cell adhesion peptides, which are often derived from interacting regions of these receptor-ligand proteins, mimic surfaces of intact proteins and, thus, have been studied as targeting agents for various payloads to certain cell targets for cancers and autoimmune diseases. Because many cytotoxic agents in the free form are often harmful to healthy cells, the use of cell adhesion peptides in targeting their delivery to diseased cells has been studied to potentially reduce required effective doses and associated harmful side-effects. In this review, multiple cell adhesion peptides from extracellular matrix and ICAM proteins were used to selectively direct drug payloads, signal-inhibitor peptides, and diagnostic molecules, to diseased cells over normal counterparts. RGD constructs have been used to improve the selectivity and efficacy of diagnostic and drug-peptide conjugates against cancer cells. From this precedent, novel conjugates of antigenic and cell adhesion peptides, called bifunctional peptide inhibitors (BPIs), have been designed to selectively regulate immune cells and suppress harmful inflammatory responses in autoimmune diseases. Similar peptide conjugations with imaging agents have delivered promising diagnostic methods in animal models of rheumatoid arthritis. BPIs have also been shown to generate immune tolerance and suppress autoimmune diseases in animal models of type-1 diabetes, rheumatoid arthritis, and multiple sclerosis. Collectively, these studies show the potential of cell adhesion peptides in improving the delivery of drugs and diagnostic agents to diseased cells in clinical settings.

Keywords

antigenic peptide; autoimmune disease; bifunctional peptide inhibitor (BPI); cell adhesion; ICAM-1; immunological synapse; integrin; LFA-1; RGD

A. Cell Adhesion Molecules and Their Roles in Biology

Cells interact with their surroundings in different ways to fulfill various functions, ranging from vital intercellular signaling to the formation of an intercellular junction of biological barriers (*i.e.*, intestinal mucosa barrier and blood-brain barrier [BBB]). Cell adhesion proteins play important roles in various diseases including, tumor metastasis, angiogenesis, tumor invasion, inflammation, thrombosis, and autoimmune diseases (*i.e.*, Type-1 diabetes (T1D), multiple sclerosis (MS), rheumatoid arthritis (RA), Crohn's) [1–4]. The changes in the expression of cell adhesion proteins on the cell surface can be used as biomarkers for a

disease state as well as for distinguishing diseased cells from normal ones. For example, the upregulation of cell adhesion receptors, $\alpha_V\beta_3$ and $\alpha_V\beta_5$ integrins, has been shown during angiogenesis in tumors [5]. Thus, cell adhesion proteins have been used as targets for (a) development of diagnostic agents, (b) drug development by inhibiting cell-adhesion process and signaling, and (c) directing drug molecules specifically to disease cells with upregulated cell adhesion proteins [3–4, 6–11].

Cell adhesion molecules (CAMs) are glycoproteins found on the cell surface and extracellular matrices (ECM) and are involved in homophilic and heterophilic protein-protein interactions during the cell adhesion process [12–13]. Homophilic interactions involve interactions between two of the same proteins, while heterophilic interactions are mediated by two different cell adhesion molecules. CAMs are responsible for (a) anchoring cells in tissues, (b) cell migrations, (c) cell-cell communications (signaling), and (d) connecting cells in the intercellular junctions of biological barriers (*i.e.*, intestinal mucosa and the BBB). There are several families of cell adhesion molecules, including (a) integrin receptors, (b) immunoglobulins, (c) cadherins, (d) selectins, and (e) extracellular matrix proteins [13–17]. The integrin family is a combination of various heterodimers of α- and β-subunits on the cell surface. Several members of the integrin family include fibronectin receptor (FNR), vitronectin receptor (VNR), very late antigen-4 (VLA-4), and lymphocyte function-associated antigen-1 (LFA-1). The integrin family has cell-signaling roles during cell migration as well as immune cell activation, including their involvement in the “outside-in” and “inside-out” signaling processes in immune cell activation and the cell adhesion process.

The members of the immunoglobulin superfamily consist of proteins that contain immunoglobulin structural repeats such as intercellular cell adhesion molecule-1 (ICAM-1), vascular cell adhesion molecule-1 (VCAM-1), and cadherins. T-cell adhesion to the antigen-presenting cell (APC) is mediated by the interaction between LFA-1 on T cell and ICAM-1 on APC. Similarly, T-cell adhesion to vascular endothelial cells can be mediated by interaction between very late antigen-4 (VLA-4) integrin receptor on T-cells and VCAM-1 on vascular endothelial cells. Immune cells can extravasate from the blood to tissue through vascular endothelium after their firm adhesion on the surface of endothelial cells mediated by ICAM-1/LFA-1 and VLA-4/VCAM-1 interactions. Prior to firm adhesion of leukocytes (*e.g.*, T cells) onto vascular endothelium, the rolling of these immune cells on the surface of vascular endothelium is mediated by the interaction of selectin on immune cells and Sialiyl-Lewis-X molecules on the cell surface vascular endothelium. The structure of the extracellular domain of E-, L-, or P-Selectin has a lectin domain, an epidermal growth factor (EGF) domain, and two complement regulatory (CR) domains.

Cadherins (*i.e.*, E-, P-, and N-cadherins) are cell surface calcium-binding glycoproteins with immunoglobulin repeats that interact in a homophilic manner to induce cell-cell adhesion in the intercellular junctions of biological barriers (*i.e.*, intestinal mucosa barrier and the blood-brain barriers). However, cadherins have also been shown to interact with integrin to mediate cell-cell adhesion. Finally, the extracellular matrix (ECM) proteins interact with integrins for anchoring cells to tissues as well as during tumor metastasis; ECM family includes fibronectin, vitronectin, fibrinogen, collagen, von Willbrand Factor, and laminin.

Several cell surface cell adhesion receptors have been shown to internalize their ligands into the cytoplasmic domain of cells. LFA-1 receptors on T cells and HL-60 leukemic cells internalize cIBR peptide derived from the ICAM-1 protein [18–20]. In a similar fashion, ICAM-1 proteins on the surface of vascular endothelial cell mediate the uptake of cLABL peptide derived from the I-domain of LFA-1 protein [21]. RGD peptides that are specifically bound to highly expressed $\alpha_V\beta_3$ and $\alpha_V\beta_5$ integrins on cancer cells have been used as peptide-drug conjugates to selectively deliver drugs and nanoparticles to cancer cells over normal cells [5–10, 22]. Thus, many cell adhesion molecules have been conjugated to drugs and imaging agents for disease treatment and diagnostics.

This review is focused on the use of cell adhesion peptides to target therapeutic, antigenic, and diagnostic molecules to cancer and immune cells with upregulated or activated cell adhesion receptors. RGD peptides have been used to deliver anticancer drugs or diagnostic agents to cancer cells with upregulated integrins such as $\alpha_V\beta_3$ and $\alpha_V\beta_5$ integrins. ICAM-1 peptides have been designed to target molecules to LFA-1 on the surface of immune cells and LFA-1 peptides to target ICAM-1 in epithelial and endothelial cells as well as immune cells. ICAM-1 peptides (*i.e.,* cIBR) have been used to deliver an anticancer drug into cancer cells and an anti-inflammatory agent to suppress T-cell activation in rheumatoid arthritis (RA) animal model. LFA-1 peptides have also been used to deliver antigenic peptides to control immune responses in animal models of autoimmune diseases (*i.e.,* RA, T1D, and MS). Cell adhesion peptides have been used to direct polymers and nanoparticles to deliver drugs and antigens to target cells. Although most conjugates of cell adhesion peptides have not yet reached clinical trials, the hope is that this review will stimulate interest in this area of research and provide background for investigating the potential of using other cell adhesion peptides for conjugates to deliver drugs and diagnostic agents.

B. Cell Adhesion Peptides

B.1. RGD Peptides Derived from ECM Proteins

Among the currently published in literature, one of the most well-studied cell adhesion peptides is RGD. The “Arg-Gly-Asp” or “RGD” sequence is found in many extracellular matrix (ECM) proteins, including fibronectin, vitronectin, fibrinogen, von Willebrand Factor, laminin, and collagen [12–15]. The RGD sequence is recognized by various integrin receptors on the cell surface for cell adhesion to ECM. The conformation of RGD sequence and the flanking residue have an important role in their recognition by specific receptor(s) in the integrin receptor family [29–30]. A cyclic RGD peptide, Integrilin®, has been used to clinically treat thrombosis because it inhibits platelet aggregation [31]. In this case, the RGD peptide binds to the integrin gpIIb/IIIa receptor on platelets and renders it unable to bind to fibrinogen for mediating platelet aggregation. Other cyclic RGD peptides have been designed for cancer treatment by inhibiting angiogenesis. These cyclic peptides selectively bind to $\alpha_V\beta_3$ and $\alpha_V\beta_5$ integrins, which are upregulated in tumors during angiogenesis [5, 29].

The recognition and selectivity of RGD peptides are governed by the distance among the positively charged guanidinium cation of the Arg residue, the carboxylic acid anion of the Asp residue, and the hydrophobicity of the flanking residue (Table 1) [32–33]. Therefore,

the peptide conformation becomes essential in imposing the structure favorable for selectivity toward a specific target integrin. The formation of a cyclic peptide delivers a degree of backbone rigidity, which limits possible conformations to those favorable for a selected integrin. Integrilin® is a cyclic peptide that is formed by a disulfide bond from two cysteine residues at the respective N- and C-terminus. Its selectivity for gpIIb/IIIa integrin receptor is due to the restricted backbone conformation [31]. In contrast, cyclic cRGDfV and cRGDyV peptides use N- to C-terminus cyclization for a rigid backbone. They are selective toward $\alpha_V\beta_3$ and $\alpha_V\beta_5$ integrins and can be delivered to solid tumor to suppress angiogenesis [10, 30, 34–36].

B.2. Non-RGD Peptide

Recently, a new non-RGD cyclic peptide called ALOS4 (cyclo-(CSSAGSLFC)) was found to bind to overexpressed integrin $\alpha_V\beta_3$ in malignant melanoma cells (Figure 1; Table 1) [37]. ALOS4 peptide has been similarly explored as a tumor targeting peptide due to its binding affinity for $\alpha_V\beta_3$ integrin. The binding site for ALOS4 on $\alpha_V\beta_3$ integrin is different from the binding site of RGD peptide [37]. However, this peptide can be used as an alternative method of delivering cytotoxic drug to cancer cells overexpressing $\alpha_V\beta_3$ integrin.

B.3. LFA-1 Derived Peptides

Another group of cell adhesion peptides found in the literature have their origins in immunological processes, particularly in the inflammatory response. The immune system defends the body against foreign antigens via the involvement of T cells and antigen-presenting cells. Interactions between ICAM-1 on the surface of APC and LFA-1 on T-cells are important not only for APC-T-cell adhesion but also as a co-stimulatory signal (Signal-2) for T-cell activation and proliferation. The antigen-specific activation of T-cells is also mediated by the T-cell receptor (TCR) recognition of antigen-major histocompatibility complex II (Ag-MHC II) presented by APCs. The TCR/Ag-MHC-II interactions can be categorized as signal-1, and the combination of signal-1 and -2 to form immunological synapse (IS) on the interface of T-cells and APC is necessary for T-cell activation and proliferation [38–40].

Inhibition of ICAM-1/LFA-1 interaction using monoclonal antibodies (mAbs) has been shown to suppress autoimmune diseases. Injections of a combination of anti-ICAM-1 and anti-CD11a mAbs twice a week for four weeks can induce immunotolerance to suppress type-1 diabetes and infiltration of islets by mononuclear cells in non-obese diabetes (NOD) mice [41]. A combination of these antibodies also prevents alograph rejection in cardiac transplantation in mice [42]. Anti-CD11a mAb (Efalizumab, Raptiva®) was previously used to treat psoriasis and it was also evaluated in phase I/II clinical trial for renal transplantation [43]. Unfortunately, this drug was pulled from the market because patients treated with this antibody developed progressive multifocal leukoencephalopathy (PML) [44]. Anti-ICAM-1 (Enlimomab) was also investigated for the treatment of rheumatoid arthritis (RA) [45–46].

X-ray crystallography of the interactions between ICAM-1 heterodimer and the I-domain was shown in Figure 2A. Two D1 domains of ICAM-1 form a homodimer, and each D1 domain binds to the I-domain of LFA-1. This interaction involves the metal ion dependent

adhesion site (MIDAS) region of I-domain. LFA-1 peptides (*i.e.*, LABL or cLABL) were derived from the I-domain of LFA-1 α-subunit where their sequence is located in the interface region of binding between I-domain and D1 of ICAM-1 (Figure 2B). Linear LABL and/or cLABL have been shown to inhibit ICAM-1/LFA-1-mediated homotypic T-cell adhesion [47–48] as well as heterotypic T-cell adhesion to Caco-2 epithelial cell monolayer [49–51]. cLABL can also inhibit binding of the anti-ICAM-1 antibody to ICAM-1 on Molt-3 T-cells, suggesting that it binds to ICAM-1. Fluorescence-labeled cLABL peptide is also internalized by ICAM-1 into Molt-3 T-cells and Caco-2 cell monolayers, indicating that it has a potential for targeting drugs to ICAM-1-expressing cells [21]. Although LABL peptide was designed using information from residue mutation studies of the I-domain prior to the availability of the X-ray structure of I-domain/ICAM-1 complex, it is interesting to find that the sequence of LABL is located within the MIDAS region of the I-domain, and at the binding interface with ICAM-1 [52]. This correlation is one of many examples affirming the value of structural elucidations of protein-protein interactions in designing promising peptides of interest.

B.4. ICAM-1 Derived Peptide

Several linear and cyclic peptides designed from the sequences of the D1 of ICAM-1 can inhibit ICAM-1/LFA-1-mediated T-cell adhesion. Both IE and IB peptides were derived from D1 of ICAM-1. Analysis of the crystal structure of the ICAM-1/I-domain complex shows that the IE peptide epitope resides in the interface between D1 of ICAM-1 and the MIDAS region of I-domain of LFA-1 (Figure 2C). In contrast, epitope for the IB peptide was found in the interface of ICAM-1/ICAM-1 homodimer (Figure 2D). The IE peptide and its cyclic peptide derivatives (*i.e.*, cIEL, cIEC, and cIER) were observed to enhance binding of anti-CD11a mAb binding to LFA-1 on T-cells, while they inhibit ICAM-1/LFA-1 T-cell adhesion. In contrast, IB peptide and its cyclic derivatives (*i.e.*, cIBL, cIBC, and cIBR) block the binding of anti-CD11a mAb to LFA-1 and also inhibit ICAM-1/LFA-1-mediated T-cell adhesion [47–48, 53]. FITC-labeled cIBR peptide has been shown to colocalize with antibody to the β-subunit (R15.7 mAb) of LFA-1 on SKW-3 T-cells, which is detected with R-phycoerythrin (PE)-labeled goat antimouse secondary antibody, suggesting that cIBR binds to LFA-1 [18]. However, X-ray crystal structure of the I-domain/ICAM-1 complex showed that the cIBR sequence was at the homodimer region of ICAM-1 not at the interface of I-domain/ICAM-1. cIBR peptide inhibits binding of various mAbs to the MIDAS and IDAS regions of the I-domain [53]. NMR binding studies between cIBR peptide and I-domain indicate that cIBR peptide binds to the IDAS region of the I-domain [54]. Thus, the hypothesis is that binding of cIBR to the IDAS region of I-domain induces the conformational change, which inhibits I-domain binding to ICAM-1 and to anti-I-domain mAbs.

C. General Principle of Peptide-Drug Conjugates (PDC)

Peptide-drug conjugates (PDC) have been developed to target drugs and radioisotopes to specific cells for therapeutic and diagnostic purposes [4, 23]. This method is similar to antibody-drug conjugates (ADC), which have been successfully used to treat cancer [24–27]. For example, Kadcycla® and Adcetris® are antibody-drug conjugates on the market that

are currently used for treating cancer patients [27]. The underlying principle is to utilize the specific binding property of the targeting peptide to unusually upregulated receptors on the surface of diseased cells compared to normal cells. This would render the concentration of the delivered drug to be higher in diseased cells than in normal cells. The ultimate aim for PDC is to be selective for diseased cells, consequently lowering the occurrence of drug side-effects with the conjugates, compared with the sole parent drugs in patients.

PDC has three fundamental components: 1) the targeting peptide, 2) the linker, and 3) the "drug payload" [23, 28]. The peptide has a function to direct the drug to a specific type of cell. It is often that the peptide segment of the PDC binds to the target receptor on the cell surface followed by PDC internalization into intracellular space via receptor-mediated endocytosis. The PDC enters the early endosomes, then moves to late endosomes and, finally, to lysosomes. The peptide portion on the PDC is degraded in the lysosomes, consequently releasing the drug intracellularly to exert its activity. The linker between peptide and drug can be designed as either fixed or cleavable to control the drug release kinetics at the desired site (*i.e.,* target cells or tissue). The release of the drug payload from the linker can be accomplished enzymatically or via a change in pH inherent to the cellular compartments in intracellular spaces of targeted cells. However, the linker has to be sufficiently stable in the systemic circulation and easily cleaved only when the PDC reaches the target cells; thus, the drug should not be prematurely released from the PDC prior to reaching its target cell or tissue.

D. Cell Adhesion Peptide-Drug Conjugates (PDC)

D.1. RGD-Drug Conjugates for Therapy

Many cytotoxic anti-cancer agents remain unviable for widespread clinical use because of harmful side effects resulting from their non-selective delivery between normal and cancer cells. One good example is paclitaxel (PTX), which is an effective cytotoxic anti-cancer drug that targets microtubule formation inside cancer cells [55]. As earlier described, one of the hallmarks of angiogenesis in tumors is the overexpression of the $\alpha_V\beta_3$ integrin, to which certain RGD peptides selectively bind over other integrins on normal cells [8, 29, 34]. PTX was then conjugated to RGD peptide in an intent to enhance its targeting to tumor cells and to overcome some of its drawbacks such as low solubility and systemic toxicity [55]. In this case, PTX was conjugated to bivalent and tetravalent RGD-based integrin ligands. While most RGD constructs employed in literature resemble the RGDfK construct of Cilengitide (Table 1), this study utilized a unique cyclic RGD pentapeptide construct, which incorporated 1-aza-1-bicycloalkane amino acids (Figure 3) [10, 55]. Single and multiple units of cyclic RGD were conjugated to the PTX payload via a triazole ring linkage, which were subsequently connected to ethylene glycol units by an amide function (Figure 3A) [55]. Mono-, bi-, tetravalent conjugates of RGD-PTX conjugates have been shown to inhibit binding of vitronectin to $\alpha_V\beta_3$ integrin receptor with relative inhibitory activities observed to be highest with tetravalent > bivalent > monovalent RGD-constructs [55]. The bivalent RGD-PTX showed cell selectivity toward IGROV-1 and IGROV-1/Pt1 ovarian cells, compared with the other conjugates. Bivalent RGD-PTX also showed a similar activity as PTX in suppressing tumor growth of xenografted IGROV-1/Pt1 tumor.

In order to similarly improve their therapeutic index by enhancing targeted delivery to tumor cells, both camptothecin (CPT) and chlorambucil (CLB) were conjugated to RGDfK using a bi-forked linker (Figure 3B) [56]. The overall intent was to create an RGD-targeted "double-drug attack", which would both be more potent and less likely to allow the tumor to develop any adequate drug resistance [56]. CPT is a very potent inhibitor of topoisomerase I enzyme; unfortunately, CPT has off-target cytotoxicity and poor solubility [56]. On the other hand, CLB is a DNA alkylator and an established anti-leukemic drug. *In vitro*, CLB was observed to be relatively inactive in its free form against melanoma and non-small cell lung cancer cell lines. However, conjugation of CLB to the carrier peptide via an amide- or ester-bonded linker with the lysine residue of RGDfK recovered its "activity" against murine leukemic cells [56]. Unlike the multimeric RGD construct, the enhanced cytotoxicity of this dual-drug conjugate was achieved through modifications of the payload component. Variations in the drug linkages were designed to achieve a sequential release of the drug upon reaching its target as directed by the RGD component. Relative stabilities of the varied drug-linked constructs were assessed across different pHs (ranging from physiologic to acidic) in order to survey their drug release profiles in the simulated environments of their tumor targets. Further bio-stability evaluations of these constructs were done in murine liver homogenate, confirming that although all constructs degraded, only conjugates with the carbamate and ester drug-linked functionalities showed the release of the free drug. This is in contrast to the construct with the amide-linked payload, which decomposes within minutes in the enzymatic environment without releasing the free drug.

Relative cytotoxicities of the mono and dual drug conjugates were evaluated against free-CLB/CPT *in vitro* using $\alpha_V\beta_3$-overexpressing B16F10 (human non-small cell lung carcinoma), H1299 (murine melanoma), and $\alpha_V\beta_3$-negative HEK (human embryonic kidney) cell-lines. *In vitro* growth inhibition assays revealed that bi-loaded CPT conjugate was more potent than mono-loaded counterparts and free-CPT. Furthermore, although growth inhibition data also showed that mixtures of free-CLB/CPT mixtures were cytotoxic in all cell lines, the dual-drug RGD construct showed the greatest cytotoxicities against $\alpha_V\beta_3$ overexpressing cell-lines (*i.e.*, human non-small cell lung carcinoma and murine melanoma) than mono-drug conjugates and mixtures of free-CPT/CLB. Even more remarkable are the differences in cytotoxicity when ratios between "targeted" to "off-target" IC_{50}s are compared, thus showing the potential of the RGD-construct in reducing off-target (*i.e.*, non-$\alpha_V\beta_3$ overexpressing cell) toxicities in next-generation CPT and CLB therapies.

W22 PDC is a conjugate between cyclo(RGDyK) and PD0325901, using a PEG-succinate linker. W22 is aimed at treating glioblastoma in the central nervous system (CNS) (Figure 3C) [57]. PD0325901 is a potent inhibitor of mitogen-activated protein kinase-1/2 (MEK1/2) – an important signaling key player during receptor tyrosine kinase (RTK) activation via extracellular signal-regulated kinase (ERK) pathway. Because RTK is upregulated in glioblastoma, inhibition of MEK1/2 activity suppresses RTK activation to inhibit glioblastoma growth. Unfortunately, intracellular delivery of PD0325901 is not efficient. Thus, W22 PDC was designed to improve targeting and drug-uptake to glioblastoma. The drug is released via cleavage of the ester bond between PD0325901 and the linker [57]. *In vitro*, the W22 PDC was more active in $\alpha_V\beta_3$ expressing U87MG cancer cells than A549 control cells. It has a higher efficacy than PD0325901 alone in U87MG and U251MG cells,

which are cell lines derived from glioblastoma. The glioblastoma tumor suppression *in vivo* was observed to be slightly better when the animals were treated with W22 PDC compared with controls PD0325901 or RGD-PEG+PD0325901. It was confirmed that the W22's mechanism of action is via suppression of the pERK1/2 expression. Furthermore, results indicate that the RGD peptide can improve the selectivity and uptake of PD0325901 in glioblastoma cells *in vitro* and *in vivo*.

A novel "photolabile switch" has been incorporated into the cRGDfK peptide component of a PDC (Figure 3D). In this construct, the lysine residue is conjugated via an amide bond to a ruthenocene complex, which serves as the payload toxic drug (component). In addition, the Asp residue of the RGD sequence is derivatized with a dicyanocoumarin protecting group (DEAdcCE) via an ester bond – resulting in a photo cleavable "cage" for the RGD component [58]. Due to the protection of the Asp residue, this RGD peptide will not be recognized by the target integrin receptor. Thus, the activity of this PDC is initiated by the cleavage of the ester bond between the Asp residue and the photosensitive DEAdcCE moiety. After the release of DEAdcCE moiety using a biologically compatible green light, the RGD sequence will be active for integrin recognition and will accordingly deliver the payload to its intended cancer target. Because the required "activating" green light has a much longer wavelength than UV wavelengths, it offers a safer alternative to previously reported photolytic constructs requiring UV light [58]. Furthermore, a methyl group near the cleavable ester bond between the caging group and the RGD-Drug construct has been reported to provide a vital structural feature that minimizes the unfavorable aspartimide forming side-reaction in its synthesis [58]. This methyl group perhaps may even contribute to the increased stability of this ester bond in physiological conditions, where the construct has not yet been reported to be tested [58]. Nonetheless, an RGD-based prodrug that is photoactivated by a biologically compatible green light presents a safe and novel addition to the growing examples of cell-adhesion peptide-based drug delivery.

D.2. RGD Peptide Conjugates for Diagnostics

Because of the ongoing success of RGD peptide conjugates in targeting drugs, the RGD conjugates have also been designed as diagnostic agents to localize cancer cells within the tissue. RGD peptides can be labeled with radioisotopes, near IR (NIR) dyes, and magnetic resonance imaging (MRI) contrast agents. As an example, cyclic RGDfK was linked to a fusion of human serum albumin and tissue inhibitor of metalloproteinase 2 (HSA-TIMP2) to make RGD-HSA-TIMP2 (Figure 3E) [59]. ^{68}Ga-NOTA- and ^{123}I-radiolabeled were incorporated to RGD-HSA-TIMP2 for cancer diagnostics that can be observed by positron emission tomography (PET) and single photon emission computed tomography (SPECT). *In vitro*, RGD-HSA-TIMP2 was engulfed more efficiently (91%) than HSA-TIMP2 (45%) by U87MG cancer cells due to the recognition of the RGD peptide [59]. RGD-HSA-TIMP2 also suppressed the proliferation of U87MG cancer cells better than HSA-TIMP2. Uptake of ^{68}Ga-NOTA-RGD-HSA-TIMP2 is higher in U87MG cells than in C6 cells, and its uptake by U87MG cells can be inhibited by free RGD peptide in solution. This suggests that the uptake of the conjugate is mediated by the recognition of RGD peptide by $\alpha_V\beta_3$ integrins on U87MG cancer cells. The uptake of ^{123}I-RGD-HSA-TIMP2 was reported to be higher than ^{123}I-HSA-TIMP2 by xenografts of human glioma cancer cells in nude mice, as detected by

SPECT; however, the images were not of good quality [59]. On the other hand, PET showed a good quality image of tumor xenograft using ^{68}Ga-NOTA-RGD-HSA-TIMP2, with no ^{68}Ga-NOTA-HSA-TIMP2 image detected in the tumor.

In rheumatoid arthritis (RA), angiogenesis to increase vascularization was observed in the synovium along with the increase in the expression of $\alpha_V\beta_3$ integrins [60]. Thus,^{99m}Tc (HYNIC-3PRGD$_2$)(tricine) called TPPTS is a cyclic RGD peptide dimer with radioisotope ^{99m}Tc. TPPTS has been utilized to detect the upregulation of $\alpha_V\beta_3$ integrins in endothelium during inflammation in RA using the SPECT system [60]. In this study, adjuvant induced RA in Sprague–Dawley rat was used as an animal model. After 30 min of TPPTS injection, the compound was observed around the rat arthritic ankles. This agent was also observed in various other organs, including bladder, kidneys, and liver. There was a linear correlation between the expression of $\alpha_V\beta_3$ integrin and the deposition of TPPTS in the arthritic ankles [60]. Furthermore, the amount of TPPTS was significantly higher in the arthritic ankles than untargeted control imaging agents with no RGD peptide. These results indicate that the high TPPTS deposition is due to binding of RGD peptide to upregulated $\alpha_V\beta_3$ integrin and has potential use as a diagnostic agent for RA

D.3. Non-RGD Peptide Conjugates

Recently, ALOS4 has been discovered as a new non-RGD cyclic peptide [Cyclo1,9(CSSAGSLFC)] that also binds to the $\alpha_V\beta_3$ integrin receptor. ALOS4 was conjugated to fluorescein isothiocyanate (FITC) via a γ-aminobutyric acid (GABA) linker, to make FITC-GABA-ALOS4 [37]. This molecule was engulfed by WM-266-4 melanoma cells via binding to upregulated $\alpha_V\beta_3$ integrins, as detected by FACScan [37]. The high deposition of FITC-GABA-ALOS4 was found at the tumor xenograft of WM-266-4 melanoma cells in nude mice, indicating tumor targeting by ALOS4 peptide. The peptide was then conjugated to camptothecin (CPT) to make CPT-GABA-ALOS4, and the cytotoxicity of CPT-GABA-ALOS4 was evaluated in WM-266-4 metastatic melanoma cells and non-malignant human kidney HEK-293 cells. The results showed that CPT-GABA-ALOS4 killed WM-266-4 cells in a dose-dependent manner to as much as 70% at 10 μM. In contrast, it only killed 30% of non-malignant HEK-293 with the same dose [37]. Because non-malignant HEK-293 do not overexpress $\alpha_V\beta_3$ integrin on their cell surfaces, the results suggest that selectivity of ALOS constructs for WM-266-4 over HEK-293 cells are due to the overexpression of $\alpha_V\beta_3$ integrins on WM-266-4 cells.

CPT-GABA-ALOS4 also shows a remarkable contrast in cancer-specific cytotoxicity compared with free CPT and two other cytotoxic drugs. In addition, the free CPT and two other cytotoxic drugs consistently killed considerable percentages of cell-populations in both WM-266-4 and non-malignant HEK-293. This study presents a promising non-RGD targeting peptide for the enhancement of chemo-stability and effective tumor-specific delivery of cytotoxic drugs [37].

D.4. ICAM-1 Peptide Conjugates

In the context of the immune response, cIBR peptide was derived from the sequence of ICAM-1. FITC-labeled cIBR has been shown to bind and be internalized by LFA-1 on the

surface of T-cells [18, 53]. Antibody inhibition and colocalization studies indicate that cIBR peptide binds to the I-domain of LFA-1 [53]. An NMR study shows that cIBR peptide binds at the IDAS region of the I-domain [54]. Conjugation of cIBR with methotrexate (MTX) to form MTX-cIBR has been shown to suppress rheumatoid arthritis in rat adjuvant arthritis model. In this case, conjugation to the cell adhesion/targeting peptide - cIBR lowered the toxicity of MTX [61].

D.5. Bifunctional Peptide Inhibitors (BPI)

Similar to the targeting design of RGD-conjugates, Bifunctional Peptide inhibitors (BPIs) are conjugates of an antigenic and cell adhesion peptide. They were designed to selectively alter the immune cell phenotypes from inflammatory to regulatory or suppressor cells in an antigenic-specific manner [62–63]. It is hypothesized that if BPIs suppress only a subpopulation of immune cells in an antigenic-specific manner, then BPIs can be an alternative solution to current drugs for autoimmune diseases, which normally suppress the general immune response. Suppression of the general immune response increases the risk for patients to be unable to fight pathogenic infections. For example, Tysabri® (Natalizumab) was withdrawn from the market because several treated patients developed progressive multifocal leukoencephalopathy (PML), most likely because of its suppressive effects on the general immune response rather than those associated only with the autoimmune disease [64–66]. Later, the use of Tysabri® was reinstated after providing certain precautions of its uses [67].

BPI molecule is a conjugate between a cell adhesion peptide (*i.e.*, LABL) and an antigenic peptide specific for controlling a specific subpopulation T-helper (T_h) cells that recognize the antigen [68–70]. The design of BPI is aimed at interfering with the formation of the immunological synapse (IS) during the T-cell activation and differentiation, when the T-cells bind to APC with a specific antigen-major histocompatibility complex-II (Ag-MHC-II) presentation (Figure 4A) [62–63]. It has been shown that the interaction between T-cell and APC forms IS on their interface, which resembles a “bull’s eye” structure [38–40]. IS is a cluster of Ag-MHC-II/TCR complexes (Signal-1) in the center, and a cluster of ICAM-1/LFA-1 complexes in the outer ring of the “bull’s eye”. Before the final IS is formed at the initial contact of T cell to APC, signal-2 complexes are in the center ring and the signal-1 complexes are in the outer ring to form an initial “bull’s eye”. Consequently, the two clusters of signals translocate or “trade places”, where the signal-2 complexes migrate to the outer ring, and the signal-1 complexes move to the center to form an inverted bull’s eye, which ultimately signals the inflammatory response. It was proposed that disrupting this final bull’s eye would trigger the proliferation of specific T_h cells that recognize specific antigen on the MHC-II, resulting in antigen-specific tolerance and immunosuppression.

It has also been shown that delivery of soluble antigenic peptide can induce immune-tolerance in the animal models of autoimmune diseases such as multiple sclerosis (MS), rheumatoid arthritis (RA), and Type-1 diabetes (T1D) [71–75]. It is proposed that the soluble antigenic peptide binds to immature dendritic cells (DCs) that lack CD80 and/or CD86 molecules. Therefore, the presence of MHC-II/Ag on immature DCs without any co-stimulatory signal from CD80 and/or CD86 renders naïve T-cell/DC interactions result in the

differentiation of naïve T-cells to produce regulatory T-cells (Treg) [76]. Tregs produce regulatory cytokines to suppress the activation of the inflammatory T-cells such as Th1 and Th17 and suppresses the autoimmune disease progression.

BPI molecules were designed to simultaneously bind to empty MHC-II and ICAM-1 on the surface of APC and block the formation of the IS when incoming T-cells bind to APCs labeled with BPI (Figure 4B). To accommodate BPI's simultaneous binding to MHC-II and ICAM-1, both antigenic and LABL peptides were docked to the X-ray structures of MHC-II and ICAM-1, respectively, as if these two proteins sit on the cell surface [74]. The length of the linker between the antigenic peptide and LABL peptide was measured by measuring the distance between the N-terminus and LABL peptide and the C-terminus of the antigenic peptide. The linker was initially generated by a combination of aminocaproic and glycine amino acids to accommodate simultaneous binding of both peptides to the respective target receptors. The concept of BPI was evaluated in animal models of autoimmune diseases, including T1D, MS, and RA.

D.5.1. BPI for Multiple Sclerosis—MS is an autoimmune neurodegenerative disease in which the immune cells infiltrate the central nervous systems (CNS) and degrade the myelin sheath of neuronal axons. The myelin sheath is partly composed of proteolipid proteins (PLP), myelin basic proteins (MBP), and myelin oligodendrocyte glycoproteins (MOG). During the disease progression, a subpopulation of T-cells recognize peptides from PLP, MBP, and MOG proteins as antigens. BPI has been developed as a potential treatment for MS. To evaluate the activity of BPI molecules as potential therapeutics for MS, experimental autoimmune encephalomyelitis (EAE) animal models have been extensively used as models for MS [63, 68–70]. EAE models show symptoms and neurodegeneration similar to MS. Relapsing and remitting MS (RRMS) model and chronic progressive MS (CPMS) EAE animal models have been used to evaluate potential therapeutic agents for MS.

The RRMS EAE mouse model (female SJL/J mice) can be stimulated using PLP peptide in complete Freund's adjuvant (CFA) on day 0, followed by injection of pertussis toxin on the same day and on day 2. Disease symptoms in mice start manifesting on day 9, with maximum disease exacerbation around days 13–15, followed by disease remission starting on day 20. The disease scores are low around days 30–45, reflecting disease remission. Animals show disease relapse again with high disease scores after day 45. At relapse, mice show high disease scores at day 54 and forward. PLP-BPI molecules have been shown to suppress the disease symptoms or lower the disease scores when injected on days 4, 7, and 10 with 100 nmol/injection [69–70]. PLP-BPIs suppress disease exacerbation and prevent the onset of relapse in the RRMS EAE model as a prophylactic type of treatment. PLP-BPI has been shown to induce remission during disease exacerbation faster than the control when injected at the beginning of disease exacerbation on day 11, suggesting the molecule can be used to suppress the disease progression. Finally, injections of PLP-BPI on days −11, −8, −5 as vaccine-like treatment before the stimulation of the disease on day 0 can also suppress the onset of EAE disease symptoms [80–82].

The CPMS EAE model (C57BL/6 mice) can be generated by injection of MOG peptide in CFA on day 0, followed by injections of pertussis toxin on the same day and on day 2.

Observable disease symptoms begin to manifest by day 7 and peak by day 13, with symptoms continuing at high scores without any remission. After induction of CPMS EAE in mice, MOG-BPI (100 nmol/injection) was administered on days 4, 7, and 10. Results showed continuous suppression of the disease scores until the end of the study on day 25 [83]. Multivalent antigen BPIs were also designed with both PLP and MOG peptides attached to LABL peptide to form PLP-MOG-BPI [83]. When injected into CPMS EAE mice on days 4, 7, and 10 at 100 nmol/injection, this multipeptide conjugate suppressed the disease better than MOG-BPI and MOG peptide alone. This suggests that a combination of PLP and MOG antigens in BPI can suppress T-cells that recognize both PLP and MOG. It was suggested that, due to the severity of the CPMS model, immune cells in this model also respond to antigens from PLP in addition to antigens from MOG. This is normally described as antigenic spreading. Administrations of 100 nmol/injection of PLP-MOG-BPI in RRMS EAE mice on days 4, 7, and 10 also suppress the disease symptoms significantly better than control.[83] As expected, MOG-BPI did not suppress the RRMS EAE primarily because the disease was stimulated with the PLP peptide. This suggests that BPI molecules suppress EAE in an antigene-specific manner, with MOG sensitivity being a potential hallmark of a more advanced/latter stage of the disease model than PLP.

To elucidate BPI's potential mechanisms of action, several experiments were carried out. These included evaluation of BPI's effects on: (a) cytokine production, (b) axon demyelination, and (c) blood-brain barrier (BBB) leakiness. The effects of BPI- and PBS-treatments on the inflammatory, regulatory, and suppressor cytokines were evaluated in EAE mice. BPI molecules significantly suppressed the productions of inflammatory cytokines IL-17, IL-6 and IFN-γ, compared with PBS controls [80, 82–83]. BPI-treated mice had a significantly higher production of regulatory (*i.e.*, IL-2 and IL-10) and suppressor (*i.e.*, IL-4 and IL-5) cytokines compared with that of PBS-treated ones [68–69, 80, 82–83]. These suggest that BPI alters the balance of immune cells from predominantly inflammatory to regulatory and/or suppressor phenotypes. Upon evaluation of the axon demyelination in the brain, BPI-treated EAE mice had intact myelination of their brains, while the PBS-treated EAE mice had clear demyelination of the axon. This indicates that BPIs suppress the activation of immune cells and prevent the infiltration of immune cells into the CNS. Finally, MRI was used to detect the leakiness of the BBB through the administration and detection of MRI contrast agent – Gadopentetic acid (Gd-DTPA) – in the brain [82]. Three different groups of mice were administered with Gd-DTPA: (1) normal mice, (2) EAE mice, and (3) EAE mice treated with BPI. Normal mice showed very limited deposition of Gd-DTPA in the brain, while the non-treated EAE mice had significantly higher Gd-DTPA deposition in the brain, suggesting that the BBB of EAE mice are leaky [82]. It is interesting to find that the deposition of Gd-DTPA in the brains of BPI-treated EAE mice are very low or even similar to those in the normal mice. This indicates that BPI treatments prevent the leakiness of the BBB.

D.5.2. BPI for Rheumatoid Arthritis (RA)—BPI molecules (*i.e.*, CII-BPI-1, -2, and -3) were also evaluated in collagen-induced arthritis (CIA) mouse model [73]. There were two CIA mouse models used in this study. The first model used DBA/1J mice, with the disease stimulated using bovine type II collagen in CFA on day 0, followed by a booster dose on day

21. Manifestation of arthritis disease symptoms (*i.e.*, paw swelling, inflammation) began between days 24 and 27. CII-BPI molecules (*i.e.*, CII-BPI-1, -2, and -3) and CII-1 peptide were administered on days 19, 22, and 25, at a dose of 100 nmol/injection. CII-1 peptide alone is an antigenic peptide that has been used previously to suppress RA in an animal model. MTX-cIBR conjugate has also been shown to suppress arthritis in rat adjuvant arthritis model, and in this case was used as a positive control. For the positive control group, MTX-cIBR was injected daily (5 mg/kg) for 10 days starting on day 19. Results showed that CII-BPI-1 significantly suppressed the increase in paw volumes compared with those treated with PBS [73]. CII-BPI-1 appeared to have been more potent than CII-1 peptide alone, with three injections of CII-BPI-1 having a potency similar to 10 injections of MTX-cIBR. Next, CII-2 and CII-3 peptides alone were similarly compared to their respective BPI molecules (*i.e.*, CII-BPI-2 and CII-BPI-3). CII-BPI-2 was found to be better than CII-2, CII-3, and CII-BPI-3. CII-BPI-3 had a better efficacy than CII-3 peptide alone [73].

The second CIA model used DBA1BO mice, which were stimulated with chicken collagen-II on CFA emulsion on day 0, and a booster dose on day 21. Disease symptoms began to show on day 17, and treatment was carried out with BPI on days 17, 22, and 25 (3x), or on days 17, 22, 25, and 28 (4x) [73]. This study showed that CII-BPI-2 was more potent than CII-2 peptide during the administration of 3 doses of peptides. These confirmed that BPIs were more effective than their parent antigenic peptides. The histopathology study of the joints showed that both CII-BPI-2 and CII significantly suppress the damage and inflammation in the knee joints, compared with those treated with PBS. Compared with PBS, CII-BPI-2 suppressed productions of inflammatory cytokines IL-6, IL-17, IFN-γ, IL-2, and TNF-α while enhancing the regulatory cytokines IL-10.[73] These further indicate that BPI molecules alter the balance of immune cells from inflammatory to regulatory cells.

D.5.3. BPI for Type-1 Diabetes—Type-1 diabetes (T1D) is an autoimmune disease in which β-cells in the islets of the pancreas are destroyed by the immune cells, and the disease progress is signified by infiltration of the islets by T-cells. Previously, soluble $GAD65_{208\text{-}217}$ peptide derived from residues 208–217 of glutamic acid decarboxylase 65 (GAD65) can suppress type-1 diabetes in NOD mice [77–79]. Thus, conjugation of $GAD65_{208\text{-}217}$ and LABL peptides via a linker (*e.g.*, Acp-Gly-Acp-Gly-Acp) created the GAD-BPI conjugate [74]. The linker and its length were designed for simultaneous binding of BPI to MHC-II and ICAM-1 on the surface of APC, ultimately to block the formation of IS during the activation of T-cells.

The efficacy of GAD-BPI was evaluated in non-obese diabetic (NOD) mice, in which the disease was stimulated with the $GAD65_{208–217}$ peptide in complete Freund's adjuvant (CFA) on day 0 to developed T1D [74]. GAD-BPI was injected intravenously (i.v.) into NOD mice on days 0 and 7, and the mice were sacrificed on day 8 for evaluation of T-cell infiltration of islets called insulitis. For a control group, mice were injected with PBS. The islets of mice treated with GAD-BPI were 85% normal (or 15% insulitis), while those treated with PBS only had 30% normal (or 70% insulitis). This result indicates that GAD-BPI suppressed the activation of T-cells to prevent insulitis. GAD-BPI induced the production of IL-4 producing cells.

Next, T cells isolated from both GAD-BPI- and PBS-treated T1D NOD mice were isolated, and these two groups of T-cells were evaluated in NOD.Scid mice in co-adoptive transfer experiments [74]. Two groups of NOD.Scid mice were injected with immune cells isolated from the NOD mice that have developed T1D. Then, the two groups of NOD.Scid mice were injected with T-cells isolated from GAD-BPI-treated NOD and PBS-treated mice. NOD.Scid mice (77%) that received T-cells isolated from GAD-BPI-treated mice did not have diabetes, with glucose levels below 250 mg/dL. Only 19% of NOD.Scid mice that received T-cells isolated from PBS-treated mice did not get diabetes. These results suggest that GAD-BPI can suppress the insulitis in NOD and NOD.Scid mice by suppressing T-cell activation. The study also showed that the GAD-BPI can simultaneously bind to ICAM-1 and MHC-II on B cells isolated from NOD mice. The anti-MHC-II and anti-ICAM-1 mAbs co-capping studies on B cells, after treatment with GAD-BPI and unlinked GAD+LABL peptides, showed a high probability that GAD-BPI binds simultaneously to MHC-II and ICAM-1 on the surface of B cells [74]. This also suggests that GAD-BPI can inhibit the formation of the immunological synapse and suppress T-cell activation in autoimmune diseases.

E. Peptide-Particle and Peptide-Polymer Conjugates

Overall efficacies reported on BPIs and PDCs have inspired innovations which either aim to utilize their targeting abilities, or load higher number of active BPIs or PDCs in a single pharmacological construct such as polymers and nanoparticles. Nanoparticles have been used to deliver drugs to improve drug dosing and for controlled drug release. Many nanoparticles are being developed as cancer therapeutic and diagnostic agents. There are several approved drugs in nanoparticle formulations including Doxil [84–86], DepoCyt [87], and Estrasorb [88]. For example, Doxil is a liposome formulation of doxorubicin functionalized with PEG [84–86]. Some of these particles have been targeted to a particular type of cell or tissue.

E.1. RGD-conjugated Biopolymers and Nanoparticles

Biopolymers bearing RGD peptides have been designed for tissue engineering and regeneration because RGD peptides can be used for cell recruitment and adhesion, especially for building tissues in wound healing, reconstructive surgeries, and neuronal regeneration. To exert RGD activity for integrin recognition, it is necessary for the peptide to have a distance from the polymer surface to avoid steric hindrance during their recognition by a specific integrin. It was suggested that the RGD peptide should be distanced from the polymer surface around 11 to 46 Å, using a PEG spacer for optimal interactions with integrin receptors on the cell surface [9, 89].

RGDfK peptides have been conjugated to chitosan, PEG polylactic acid (PLA), and polyethyleneimines (PEI) for delivering anticancer drugs and DNA. RGD peptide conjugated with polylactic acid (PLA) polymer (RGD-ST-NH-PEG-PLA) has been shown to induce attachment of human osteoblasts to the polymer [90]. This cell attachment can be blocked by soluble RGD peptide. In contrast, immobilized Arg-Ala-Asp (RAD) peptide attached to the polymer (RAD-ST-NH-PEG-PLA) did not initiate the attachment of human osteoblasts [90]. Taken together, the data indicate that the cell attachment of human

osteoblast cells to the polymer is due to the recognition of RGD peptide by integrin receptors on the cell surface.

As mentioned previously, liposomes have been used to deliver drugs to tumor cells, including RGDfK peptide constructs conjugated to PEG-2000 distearoylphosphatidyl-ethanolamine (DSPE), for incorporation into liposomes to target cancer cells. RGD and RAD peptides conjugated to polyethylene glycol (PEG) were incorporated into long-circulating liposomes (LCL) to make RGD-LCL and RAD-LCL. RGD-LCL shows significant binding to human umbilical vein endothelial cells (HUVEC) compared with LCL and RAD-LCL as negative controls [91]. Furthermore, binding of RGD-LCL was inhibited by soluble RGD peptide but not RAD peptide, indicating that the RGD-LCL binding to HUVEC was mediated by RGD peptide. Then, RGD-LCL was labeled with fluorescence dye Rho-PE and injected into tumor-bearing mice. The Rho-PE–labeled RGD-LCL was bound to the tumor vasculature, as observed by intravital microscopy [91]. Finally, doxorubicin-loaded liposomes (*i.e.*, LCL, RAD-LCL, RGD-LCL) were injected into mice bearing a C26 tumor. The results showed that Dox-RGD-LCL suppressed tumor growth more significantly than those treated with Dox-RAD-LCL and Dox-LCL, thus confirming the role of RGD peptide in directing liposomes to tumor cells [91].

RGD-PEG-liposomes have been developed to deliver dexamethasone phosphate to treat arthritis in adjuvant-induced arthritis in rats [92]. As earlier mentioned, upregulated $\alpha_V\beta_3$ integrins have been shown in arthritic tissues; thus, a high localization of RGD-PEG-liposomes was found in the inflamed skin of joints of lipopolysaccharide-induced rheumatoid arthritis rats [92]. RGD-PEG-liposomes carrying dexamethasone were more potent in suppressing RA than blank liposomes containing dexamethasone alone, indicating the capability of RGD peptide to target liposomes to arthritis tissues.

Carboplatin is an anticancer drug and, although it is widely used, these types of drugs are known to have low cellular uptake and to generate multi-drug resistance in cancer therapy. One way to overcome drug resistance is by formulating carboplatin in unimolecular nanoparticles with the idea that the targeted carboplatin can be released in a pH-sensitive manner [93]. In this case, a block copolymer poly(amidoamine)-*b*-poly(aspartic acid)-*b*-poly(ethylene glycol) (PAMAM-PAsp-PEG) was used as a core nanoparticle with multiple linkable arms. cRGDfC peptide was one of the linked moieties used to target the nanoparticles to cancer cells [93]. The core arm was connected to poly-aspartic acid chains in order to coordinate carboplatin on the nanoparticle through two carboxylic acid side chains of the series of Asp residues [93]. Additional arms that extend from the PAMAM core were conjugated to fluorescent dye cyanin5 (Cy5) in order to follow cell or tissue deposition of the nanoparticles. The uptake of RGD-containing nanoparticles was 3–4 fold more than nanoparticles without RGD peptide in ovarian cancer-3 (OVCAR-3) cells, indicating the role of RGD peptide and overexpression of $\alpha_V\beta_3$ integrins in the targeted nanoparticle delivery [93]. Furthermore, nanoparticles were internalized into lysosomes of the cancer cells. The pH drop resulting from the inherently acidic environment of the cancerous lysosomes protonates the carboxylic side-chains of the carboplatin-complexed poly-Asp network and releases the cytotoxic payload to its target [93]. *In vitro*, the carboplatin is released up to 88% at pH 5.5, while it is only released up to 18% at pH 7.4 by

the 50-hour time point, showing that carboplatin can be released in a targeted and controlled way in lysosomes of cancer cells. The cytotoxicity assays showed that RGD-containing carboplatin nanoparticles significantly suppress the OVCAR-3 cell viability, compared with carboplatin nanoparticles without RGD peptide and carboplatin alone [93].

E.2. Particles with Bifunctional Peptides

Recently, bifunctional peptide-targeting has been explored to improve tumor targeting and apoptosis effects. Here, nanoparticles were decorated with encapsulated docetaxel (DOC). A combination of HAV, NGRRGD, and AVPIAQK sequences was implemented in HRK-19 peptide (HAVRNGRRGDGGAVPIAQK) to target the DOC-bearing nanoparticles to tumor cells. The HAV, NGR, and RGD sequences were used to target cadherin, $\alpha_V\beta_3$ integrins, and aminopeptidase-N (CD13), respectively, on tumor blood vessels [94]. At 5 nM dose, the apoptotic index of DOC-loaded-HRK-19 peptide nanoparticles was significantly higher than DOC alone on treated A549 cancer cells. Nanoparticles decorated with HRK-19 peptide (DOC-loaded-HRK-19) penetrated xenograft tumor with high efficiency *in vivo,* with slightly better efficacy than that of drug alone, in extending animal survival [94]. The nanoparticle efficacy was significantly better than saline and HRK-19 alone in suppressing A549 tumor growth and extending animal survival [94]. DOC-loaded-HRK-19 nanoparticles also significantly suppressed pulmonary tumor metastasis of A549 cells, compared with saline and peptide alone.

E.3. LABL Conjugation to Particles for Delivery

CPP), has been conjugated to a linear LABL peptide to make the TAT-PEG-LABL conjugate [95]. The TAT peptide in the conjugate was complexed with luciferase DNA via electrostatic interactions by condensing them using calcium to form particles with a 300-nm size [95]. The LABL peptide had the role of targeting the particles to ICAM-1-bearing A549 cells for DNA internalization [95]. Upon activation of A549 lung epithelial cells with TNF-α, TAT-PEG-LABL(DNA) enhanced luciferase transfection compared with TAT-PEG(DNA), suggesting that LABL peptide targets the particles into A549 cells [95]. The TAT-PEG-LABL(DNA) transfection was also blocked by free LABL peptide and anti-ICAM-1 mAb, indicating that TAT-PEG-LABL(DNA) uptake was ICAM-1-mediated endocytosis via binding to LABL peptide on the surface of particles [95].

The surface of nanoparticles made from pluronic-F-127/PLGA was decorated with a cyclic, cLABL peptide (Cyclo-(1,12)-PenITDGEATDSGC) to produce cLABL-NP (or cLABL-Pluronic-F-17-PLGA) [96]. The uptake of cLABL-NP was higher than that of NP (2.3 fold) alone by A549 lung epithelial cells bearing the ICAM-1 receptor. Internalized within 5 min, cLABL-NP had a fast kinetic uptake [96]. Uptake of cLABL-NP, however, was inhibited by cLABL and anti-ICAM-1 mAb, suggesting that the uptake was mediated by ICAM-1 receptors on the cell surface [96]. It was suggested that the internalization of the cLABL-NP was induced by clustering of ICAM-1 to form multimeric interaction with the nanoparticles, similar to that of anti-ICAM-1 decorated nanoparticles [97–99]. The lysosome accumulation of cLABL-NP was within 1 h after incubation, compared with 2 h after incubation for blank nanoparticles. The cLABL-NP was removed from the lysosomes within 24 h and this removal was not due to a lysosomal disruption.

Similar to BPI molecules, the development of soluble antigen arrays (SAgAs; Figure 5) was inspired by a combination of the BPI concept and Dintzis' rules, which have been shown to induce immune stimulation or tolerance [100–106]. Dintzis' rules indicated that induced immune responses are influenced by particle size, solubility, flexibility, antigen valency, spacing, and binding avidity. The BPI concept showed that a conjugation of an antigenic peptide and co-stimulatory signal peptide (inhibitor) can alter immune cell phenotypes [107–108]. Thus, $SAgA_{PLP\text{-}LABL}$ molecules were designed to resemble BPI molecules containing a combination of PLP antigenic and LABL peptides linked to hyaluronic acid polymers with an 11:10 LABL:PLP peptide ratio per polymer unit (Figure 5) [103]. The SAgA molecules are soluble and small, with a size of <100kDa. The presence of multiple ligands on the polymer construct enhances avidity for dendritic cells. $SAgA_{PLP\text{-}LABL}$ delivers a multivalence of adhesion peptides, which have previously been reported to enhance cell-binding by increased avidity and to inhibit inflammatory signaling by mimicking the native clustering of bound cell-surface protein targets related to the immunological synapse. Overall features of SAgAs fulfilled good tolerogenic properties according to Dintzis' rules, and their efficacy was evaluated in the EAE animal model for MS. Compared with HA_{PLP}, HA_{LABL} and HA alone (Figure 5), $SAgA_{PLP\text{-}LABL}$ had excellent efficacy in suppressing EAE in mice; however, administration of a 1:1 mixture of homopolymers HA_{PLP} and HA_{LABL} also showed a significant disease suppression similar to that of $SAgA_{PLP\text{-}LABL}$. These results support the idea that $SAgA_{PLP\text{-}LABL}$ is a novel and effective antigenic-SIT and affirm the need for co-delivering a cell-adhesion inhibitor and an antigenic peptide to induce degrees of immunotolerance in autoimmune diseases. Because comparable protections were delivered against murine EAE by administrations of the novel $SAgA_{PLP\text{-}LABL}$, and a 1:1 mixture of HA_{PLP}+HA_{LABL}, the immunosuppressive mechanisms of both formulations remain uncertain; thus, further studies on their mechanism of action need to be explored.

In an attempt to elucidate the mechanism of action of SAgAs *in vitro*, a separate multi-peptide construct using hyaluronic acid (HA) conjugated with multiple LABL and antigenic ovalbumin (OVA) peptides was synthesized to construct $SAgA_{OVA\text{-}LABL}$ [100]. The cellular binding and uptake properties of FITC-labeled $SAgA_{OVA\text{-}LABL}$ were compared to HA_{OVA} and HA_{LABL}, using bone marrow derived dendritic cells (DC). The maturation of DC was accomplished using TNF-α. Because HA alone is a natural ligand to many cell surface receptors, observed fluorescence indicating substantial binding of unconjugated HA was expected [100]. $SAgA_{OVA\text{-}LABL}$ and HA_{LABL} both showed a considerable increase in binding to DCs compared with HA alone [100]. Because HA_{OVA} did not appear to bind efficiently to DC, it is unclear if its grafting with LABL provided the slight binding enhancement in the $SAgA_{OVA\text{-}LABL}$ construct even though it has been suggested that antigenic peptides can bind with low affinity to empty MHCs of DC. As in the previous study, the degree of T-cell proliferation was determined after co-culture with groups of DC which were initially matured, primed and pre-treated with the different HA grafts. T-cell proliferation was measured by flow cytometry after 24-hours and 7-days. Both $SAgA_{OVA\text{-}LABL}$ and HA_{LABL} grafts showed a statistically significant reduction in cells which have divided *vs.* the untreated group and the negative control of T-cells alone. It was noted that there was no significant difference between the untreated control and cell group treated with HA alone.

Because affecting T-cell proliferation can also correlate to a modified control in cytokine production, the production of TNF-α, IFN-γ, IL-4, IL-10, and IL-17 were investigated by ELISA [100]. HA and $SAgA_{OVA\text{-}LABL}$ did not show any increase in the levels of IFN-γ, IL-4, and IL-10. When compared with the untreated control, a significant reduction in TNF-α and IL-17 secretion was observed in the presence of HA and $SAgA_{OVA\text{-}LABL}$ grafts. TNF-α promotes inflammatory responses and can lead to various autoimmune and inflammatory diseases. IL-17 has likewise been associated with a wide range of similar diseases such as asthma, rheumatoid arthritis, psoriasis, and systemic sclerosis. Amounts of TNF-α in the medium of cells treated with HA, $SAgA_{OVA\text{-}LABL}$ and $SAgA_{LABL}$ were from 10.9 ng/mL (untreated) to 3.7, 4.1, and 8.2 ng/mL, respectively. IL-17 produced from untreated cells was 13.9 ng/mL, in contrast to those secreted by HA and $SAgA_{OVA\text{-}LABL}$ and $SAgA_{LABL}$-treated cells, which were below the detection limit of < 2 pg/mL. These are consistent with the significant reduction in T-cell-DC interactions observed in the presence of HA (79%), $SAgA_{LABL}$(82%), and $SAgA_{OVA\text{-}LABL}$(85%), compared with the untreated control. These results demonstrate HA graft polymers as potential inhibitors of Th17 CD4 cell differentiation and unwanted inflammatory responses in the context of autoimmune diseases.

F. Conclusions

Cell adhesion peptides have been important innovations in addressing the problem of off-target cytotoxicity and the side effects of drug molecules. Cell-adhesion peptides serve as effective targeting agents in directing diagnostic and therapeutic molecules toward diseased cells and tissues (*e.g.*, cancer and autoimmune) often through abnormally overexpressed cell adhesion receptors. By mimicking native interactions of fully intact proteins, peptide epitopes derived from protein surfaces have been used to design targeting cell adhesion peptides. Insights on viable cell adhesion sequences have far evolved from the study of primary sequences and *in vitro* inhibition and/or binding studies to more direct crystallographic and structural techniques probing vital interactions of cell adhesion proteins. Current biophysical methods to visualize locations of viable cell-adhesion epitopes on intact protein structures facilitate the mining of vital amino acid sequences and a greater understanding of viable homing peptides for disease-specific delivery of drug and diagnostic molecules. Unlike intact proteins and antibodies, cell-adhesion peptides are simpler to synthesize, isolate, and manage. The absence of any tertiary structure renders them more forgiving in storage and formulation. More importantly, their considerably smaller size allows for multiple peptide units to be conjugated to a single construct for the enhancement of both potency and selective delivery of conjugated cytotoxic molecules. In promoting immunotolerance, BPI molecules deliver antigenic peptides to specifically suppress autoimmune diseases in animal models for type-1 diabetes, rheumatoid arthritis, and multiple sclerosis. They further demonstrate additional important roles of conjugate linkers, beyond the simple function of bridging targeting and payload components of a conjugate construct. From a pharmacokinetic standpoint, conjugates have to be stable in circulation until their target cells or tissues are reached, prior to the release of the drug. Thus, various factors need to be considered in designing conjugates for cell adhesion peptides, including the conjugation methods and the length of the covalent linker to control the stability and toxicity of the construct. In any case, the range of applications presented in the reviewed

conjugate molecules demonstrate good models to be adopted for next generation therapies to be considered for clinical trials.

Acknowledgments

We would like to thank the NIH for an IRACDA postdoctoral fellowship (5K12GM063651) to MEGM and for funding our research under grant number R01-NS075374.

Abbreviations

Ac	acetyl
Acp	aminocaproic acid
ADC	antibody drug conjugates
Ag	antigen
Ag-MHC-II	antigen-majorhistocompatibility complex-II
APC	antigen-presenting cell
BBB	blood brain barrier
BPI	bifunctional peptide inhibitor
CAMs	cell adhesion molecules
CD13	aminopeptidase-N
CFA	complete Freund’s adjuvant
CIA	collagen-induced arthritis
CLB	chlorambucil
CNS	central nervous systems
CPMS	chronic progressive multiple sclerosis
CPP	cell-penetrating peptide
CPT	camptothecin
CR	complement regulatory
Cy5	cyanin5 fluorescent dye
DC	dentritic cells
DOC	docetaxel
DSPE	distearoylphosphatidylethanolamine
EAE	experimental autoimmune encephalomyelitis

ECM	extracellular matrix
EGF	epidermal growth factor
ERK	extracellular signal-regulated kinase
FITC	fluorescein isothiocyanate
FNR	fibronectin receptor
GABA	γ–aminobutyric acid
GAD65	glutamic acid decarboxylase 65
Gd-DTPA	gadopentetic acid
HA	hyaluronic acid
HEK	human embryonic kidney cells
HSA	human serum albumin
HUVEC	human umbilical vein endothelial cells
HYNIC	6-hydrazinonicotinyl
ICAM-1	intercellular cell adhesion molecule-1
IDAS	I-domain allosteric site
IFN-γ	interferon gamma
IL	interleukin
IS	immunological synapse
LCL	long circulating liposomes
LFA-1	lymphocyte function-associated antigen-1
MAPK/MEK1/2	mitogen activated protein kinase-1/2
MBP	myelin basic protein
MHC-II	major histocompatibility complex-II
MIDAS	metal-ion dependent adhesion site
MOG	myelin oligodendrocyte glycoprotein
MRI	magnetic resonance imaging
MS	multiple sclerosis
MTX	methotrexate
NIR	near infrared

NOD	non-obese diabetes
NP	nanoparticle
OVA	ovalbumin
OVCAR-3	ovarian cancer-3 cells
PAMAM	poly(amidoamine)-*b*-poly(aspartic acid)-*b*-poly(ethylene glycol)
PBS	phosphate buffered saline
PDC	peptide drug conjugates
PEG/Peg	polyethylene glycols
PEG_4	15-amino-4,7,10,13-tetraoxapentadecanoic acid
PEI	polyethyleneimines
Pen	penicillamine
PET	positron emission tomography
PLA	polylactic acid
PLGA	poly(lactic-co-glycolic acid)
PLP	proteolipid protein
PML	progressive multifocal leukoencephalopathy
PTX	paclitaxel
RA	rheumatoid arthritis
RAD	Arg-Ala-Asp
RGD	Arg-Gly-Asp
RRMS	relapse remitting multiple sclerosis
RTK	receptor tyrosine kinase
SAgAs	soluble antigen arrays
SPECT	single photon emission computed tomography
T1D	type-1 diabetes
TAT	trans-activating transcriptor
TCR	T-cell receptor
T_h	T-helper cell

TIMP2	tissue inhibitor of metalloproteinase 2
TNF-α	tumor necrosis factor alpha
TPPTS	trisodium triphenylphosphine-3,3′,3′-trisulfonate
Treg	regulatory T-cells
TXT	taxotere
VCAM-1	vascular cell adhesion molecule-1
VLA-4	very late antigen-4
VNR	victronectin receptor.

H. References

1. Golias C, Tsoutsi E, Matziridis A, Makridis P, Batistatou A, Charalabopoulos K. Review. Leukocyte and endothelial cell adhesion molecules in inflammation focusing on inflammatory heart disease. In Vivo. 2007; 21(5):757–69. [PubMed: 18019409]
2. Huveneers S, Truong H, Danen HJ. Integrins: signaling, disease, and therapy. Int J Radiat Biol. 2007; 83(11–12):743–51. [PubMed: 17852562]
3. Yusuf-Makagiansar H, Anderson ME, Yakovleva TV, Murray JS, Siahaan TJ. Inhibition of LFA-1/ICAM-1 and VLA-4/VCAM-1 as a therapeutic approach to inflammation and autoimmune diseases. Med Res Rev. 2002; 22(2):146–67. [PubMed: 11857637]
4. Dunehoo AL, Anderson M, Majumdar S, Kobayashi N, Berkland C, Siahaan TJ. Cell adhesion molecules for targeted drug delivery. J Pharm Sci. 2006; 95(9):1856–72. [PubMed: 16850395]
5. Meyer A, Auernheimer J, Modlinger A, Kessler H. Targeting RGD recognizing integrins: drug development, biomaterial research, tumor imaging and targeting. Curr Pharm Des. 2006; 12(22): 2723–47. [PubMed: 16918408]
6. Gaertner FC, Kessler H, Wester HJ, Schwaiger M, Beer AJ. Radiolabelled RGD peptides for imaging and therapy. Eur J Nucl Med Mol Imaging. 2012; 39(Suppl 1):S126–38. [PubMed: 22388629]
7. Goligorsky MS, Noiri E, Kessler H, Romanov V. Therapeutic effect of arginine-glycine-aspartic acid peptides in acute renal injury. Clin Exp Pharmacol Physiol. 1998; 25(3–4):276–9. [PubMed: 9590583]
8. Heckmann D, Kessler H. Design and chemical synthesis of integrin ligands. Methods Enzymol. 2007; 426:463–503. [PubMed: 17697896]
9. Hersel U, Dahmen C, Kessler H. RGD modified polymers: biomaterials for stimulated cell adhesion and beyond. Biomaterials. 2003; 24(24):4385–415. [PubMed: 12922151]
10. Mas-Moruno C, Rechenmacher F, Kessler H. Cilengitide: the first anti-angiogenic small molecule drug candidate design, synthesis and clinical evaluation. Anticancer Agents Med Chem. 2010; 10(10):753–68. [PubMed: 21269250]
11. Anderson ME, Siahaan TJ. Targeting ICAM-1/LFA-1 interaction for controlling autoimmune diseases: designing peptide and small molecule inhibitors. Peptides. 2003; 24(3):487–501. [PubMed: 12732350]
12. Pierschbacher MD, Ruoslahti E. Cell attachment activity of fibronectin can be duplicated by small synthetic fragments of the molecule. Nature. 1984; 309(5963):30–3. [PubMed: 6325925]
13. Ruoslahti E, Hayman EG, Pierschbacher MD. Extracellular matrices and cell adhesion. Arteriosclerosis. 1985; 5(6):581–94. [PubMed: 2416306]
14. Pierschbacher MD, Hayman EG, Ruoslahti E. The cell attachment determinant in fibronectin. J Cell Biochem. 1985; 28(2):115–26. [PubMed: 3908463]

15. Ruoslahti E, Pierschbacher MD. New perspectives in cell adhesion: RGD and integrins. Science. 1987; 238(4826):491–7. [PubMed: 2821619]
16. Humphries MJ. Integrin structure. Biochem Soc Trans. 2000; 28(4):311–39. [PubMed: 10961914]
17. Weis WI. Cadherin structure: a revealing zipper. Structure. 1995; 3(5):425–7. [PubMed: 7663938]
18. Anderson ME, Siahaan TJ. Mechanism of binding and internalization of ICAM-1-derived cyclic peptides by LFA-1 on the surface of T cells: a potential method for targeted drug delivery. Pharm Res. 2003; 20(10):1523–32. [PubMed: 14620502]
19. Majumdar S, Kobayashi N, Krise JP, Siahaan TJ. Mechanism of internalization of an ICAM-1-derived peptide by human leukemic cell line HL-60: influence of physicochemical properties on targeted drug delivery. Mol Pharm. 2007; 4(5):749–58. [PubMed: 17680719]
20. Majumdar S, Tejo BA, Badawi AH, Moore D, Krise JP, Siahaan TJ. Effect of modification of the physicochemical properties of ICAM-1-derived peptides on internalization and intracellular distribution in the human leukemic cell line HL-60. Mol Pharm. 2009; 6(2):396–406. [PubMed: 19296614]
21. Yusuf-Makagiansar H, Siahaan TJ. Binding and internalization of an LFA-1-derived cyclic peptide by ICAM receptors on activated lymphocyte: a potential ligand for drug targeting to ICAM-1-expressing cells. Pharm Res. 2001; 18(3):329–35. [PubMed: 11442273]
22. Arap W, Pasqualini R, Ruoslahti E. Chemotherapy targeted to tumor vasculature. Curr Opin Oncol. 1998; 10(6):560–5. [PubMed: 9818236]
23. Majumdar S, Siahaan TJ. Peptide-mediated targeted drug delivery. Med Res Rev. 2012; 32(3):637–58. [PubMed: 20814957]
24. de Goeij BE, Lambert JM. New developments for antibody-drug conjugate-based therapeutic approaches. Curr Opin Immunol. 2016; 40:14–23. [PubMed: 26963132]
25. Kim EG, Kim KM. Strategies and Advancement in Antibody-Drug Conjugate Optimization for Targeted Cancer Therapeutics. Biomol Ther (Seoul). 2015; 23(6):493–509. [PubMed: 26535074]
26. Sassoon I, Blanc V. Antibody-drug conjugate (ADC) clinical pipeline: a review. Methods Mol Biol. 2013; 1045:1–27. [PubMed: 23913138]
27. Sau S, Alsaab HO, Kashaw SK, Tatiparti K, Iyer AK. Advances in antibody-drug conjugates: A new era of targeted cancer therapy. Drug Discov Today. 2017
28. Ma L, Wang C, He Z, Cheng B, Zheng L, Huang K. Peptide-Drug Conjugate: A Novel Drug Design Approach. Curr Med Chem. 2017
29. Gurrath M, Muller G, Kessler H, Aumailley M, Timpl R. Conformation/activity studies of rationally designed potent anti-adhesive RGD peptides. Eur J Biochem. 1992; 210(3):911–21. [PubMed: 1483474]
30. Pfaff M, Tangemann K, Muller B, Gurrath M, Muller G, Kessler H, Timpl R, Engel J. Selective recognition of cyclic RGD peptides of NMR defined conformation by alpha IIb beta 3, alpha V beta 3, and alpha 5 beta 1 integrins. J Biol Chem. 1994; 269(32):20233–8. [PubMed: 8051114]
31. Tcheng JE. Impact of eptifibatide on early ischemic events in acute ischemic coronary syndromes: a review of the IMPACT II trial. Integrilin to Minimize Platelet Aggregation and Coronary Thrombosis. Am J Cardiol. 1997; 80(4A):21B–28B. [PubMed: 9205014]
32. Marinelli L, Lavecchia A, Gottschalk KE, Novellino E, Kessler H. Docking studies on alphavbeta3 integrin ligands: pharmacophore refinement and implications for drug design. J Med Chem. 2003; 46(21):4393–404. [PubMed: 14521404]
33. Marinelli L, Meyer A, Heckmann D, Lavecchia A, Novellino E, Kessler H. Ligand binding analysis for human alpha5beta1 integrin: strategies for designing new alpha5beta1 integrin antagonists. J Med Chem. 2005; 48(13):4204–7. [PubMed: 15974570]
34. Dechantsreiter MA, Planker E, Matha B, Lohof E, Holzemann G, Jonczyk A, Goodman SL, Kessler H. N-Methylated cyclic RGD peptides as highly active and selective alpha(V)beta(3) integrin antagonists. J Med Chem. 1999; 42(16):3033–40. [PubMed: 10447947]
35. Higuchi T, Bengel FM, Seidl S, Watzlowik P, Kessler H, Hegenloh R, Reder S, Nekolla SG, Wester HJ, Schwaiger M. Assessment of alphavbeta3 integrin expression after myocardial infarction by positron emission tomography. Cardiovasc Res. 2008; 78(2):395–403. [PubMed: 18256073]
36. Schottelius M, Laufer B, Kessler H, Wester HJ. Ligands for mapping alphavbeta3-integrin expression *in vivo*. Acc Chem Res. 2009; 42(7):969–80. [PubMed: 19489579]

37. Redko B, Tuchinsky H, Segal T, Tobi D, Luboshits G, Ashur-Fabian O, Pinhasov A, Gerlitz G, Gellerman G. Toward the development of a novel non-RGD cyclic peptide drug conjugate for treatment of human metastatic melanoma. Oncotarget. 2017; 8(1):757–768. [PubMed: 27768593]
38. Grakoui A, Bromley SK, Sumen C, Davis MM, Shaw AS, Allen PM, Dustin ML. The immunological synapse: a molecular machine controlling T cell activation. Science. 1999; 285(5425):221–7. [PubMed: 10398592]
39. Dustin ML, Shaw AS. Costimulation: building an immunological synapse. Science. 1999; 283(5402):649–50. [PubMed: 9988658]
40. Davis MM, Wulfing C, Krummel MF, Savage PA, Xu J, Sumen C, Dustin ML, Chien YH. Visualizing T-cell recognition. Cold Spring Harb Symp Quant Biol. 1999; 64:243–51. [PubMed: 11232292]
41. Yoneda R, Yokono K, Nagata M, Tominaga Y, Moriyama H, Tsukamoto K, Miki M, Okamoto N, Yasuda H, Amano K, Kasuga M. CD8 cytotoxic T-cell clone rapidly transfers autoimmune diabetes in very young NOD and MHC class I-compatible scid mice. Diabetologia. 1997; 40(9): 1044–52. [PubMed: 9300241]
42. Isobe M, Yagita H, Okumura K, Ihara A. Specific acceptance of cardiac allograft after treatment with antibodies to ICAM-1 and LFA-1. Science. 1992; 255(5048):1125–7. [PubMed: 1347662]
43. Vincenti F, Mendez R, Pescovitz M, Rajagopalan PR, Wilkinson AH, Butt K, Laskow D, Slakey DP, Lorber MI, Garg JP, Garovoy M. A phase I/II randomized open-label multicenter trial of efalizumab, a humanized anti-CD11a, anti-LFA-1 in renal transplantation. Am J Transplant. 2007; 7(7):1770–7. [PubMed: 17564637]
44. Berger JR, Houff SA, Major EO. Monoclonal antibodies and progressive multifocal leukoencephalopathy. MAbs. 2009; 1(6):583–9. [PubMed: 20073129]
45. Kavanaugh AF, Davis LS, Nichols LA, Norris SH, Rothlein R, Scharschmidt LA, Lipsky PE. Treatment of refractory rheumatoid arthritis with a monoclonal antibody to intercellular adhesion molecule 1. Arthritis Rheum. 1994; 37(7):992–9. [PubMed: 7912930]
46. Kavanaugh AF, Davis LS, Jain RI, Nichols LA, Norris SH, Lipsky PE. A phase I/II open label study of the safety and efficacy of an anti-ICAM-1 (intercellular adhesion molecule-1; CD54) monoclonal antibody in early rheumatoid arthritis. J Rheumatol. 1996; 23(8):1338–44. [PubMed: 8856611]
47. Tibbetts SA, Chirathaworn C, Nakashima M, Jois DS, Siahaan TJ, Chan MA, Benedict SH. Peptides derived from ICAM-1 and LFA-1 modulate T cell adhesion and immune function in a mixed lymphocyte culture. Transplantation. 1999; 68(5):685–92. [PubMed: 10507489]
48. Tibbetts SA, Seetharama Jois D, Siahaan TJ, Benedict SH, Chan MA. Linear and cyclic LFA-1 and ICAM-1 peptides inhibit T cell adhesion and function. Peptides. 2000; 21(8):1161–7. [PubMed: 11035201]
49. Yusuf-Makagiansar H, Makagiansar IT, Hu Y, Siahaan TJ. Synergistic inhibitory activity of alpha- and beta-LFA-1 peptides on LFA-1/ICAM-1 interaction. Peptides. 2001; 22(12):1955–62. [PubMed: 11786177]
50. Yusuf-Makagiansar H, Makagiansar IT, Siahaan TJ. Inhibition of the adherence of T-lymphocytes to epithelial cells by a cyclic peptide derived from inserted domain of lymphocyte function-associated antigen-1. Inflammation. 2001; 25(3):203–14. [PubMed: 11403212]
51. Yusuf-Makagiansar H, Yakovleva TV, Tejo BA, Jones K, Hu Y, Verkhivker GM, Audus KL, Siahaan TJ. Sequence recognition of alpha-LFA-1-derived peptides by ICAM-1 cell receptors: inhibitors of T-cell adhesion. Chem Biol Drug Des. 2007; 70(3):237–46. [PubMed: 17718718]
52. Shimaoka M, Xiao T, Liu JH, Yang Y, Dong Y, Jun CD, McCormack A, Zhang R, Joachimiak A, Takagi J, Wang JH, Springer TA. Structures of the alpha L I domain and its complex with ICAM-1 reveal a shape-shifting pathway for integrin regulation. Cell. 2003; 112(1):99–111. [PubMed: 12526797]
53. Anderson ME, Tejo BA, Yakovleva T, Siahaan TJ. Characterization of binding properties of ICAM-1 peptides to LFA-1: inhibitors of T-cell adhesion. Chem Biol Drug Des. 2006; 68(1):20–8. [PubMed: 16923022]

54. Zimmerman T, Oyarzabal J, Sebastian ES, Majumdar S, Tejo BA, Siahaan TJ, Blanco FJ. ICAM-1 peptide inhibitors of T-cell adhesion bind to the allosteric site of LFA-1. An NMR characterization. Chem Biol Drug Des. 2007; 70(4):347–53. [PubMed: 17868072]
55. Bianchi A, Arosio D, Perego P, De Cesare M, Carenini N, Zaffaroni N, De Matteo M, Manzoni L. Design, synthesis and biological evaluation of novel dimeric and tetrameric cRGD-paclitaxel conjugates for integrin-assisted drug delivery. Org Biomol Chem. 2015; 13(27):7530–41. [PubMed: 26074454]
56. Gilad Y, Noy E, Senderowitz H, Albeck A, Firer MA, Gellerman G. Dual-drug RGD conjugates provide enhanced cytotoxicity to melanoma and non-small lung cancer cells. Biopolymers. 2015
57. Hou J, Diao Y, Li W, Yang Z, Zhang L, Chen Z, Wu Y. RGD peptide conjugation results in enhanced antitumor activity of PD0325901 against glioblastoma by both tumor-targeting delivery and combination therapy. Int J Pharm. 2016; 505(1–2):329–40. [PubMed: 27085642]
58. Gandioso A, Cano M, Massaguer A, Marchan V. A Green Light-Triggerable RGD Peptide for Photocontrolled Targeted Drug Delivery: Synthesis and Photolysis Studies. J Org Chem. 2016; 81(23):11556–11564. [PubMed: 27934458]
59. Wang F, Li Y, Shen Y, Wang A, Wang S, Xie T. The functions and applications of RGD in tumor therapy and tissue engineering. Int J Mol Sci. 2013; 14(7):13447–62. [PubMed: 23807504]
60. Huang C, Zheng Q, Miao W. Study of novel molecular probe 99mTc-3PRGD2 in the diagnosis of rheumatoid arthritis. Nucl Med Commun. 2015; 36(12):1208–14. [PubMed: 26352213]
61. Majumdar S, Anderson ME, Xu CR, Yakovleva TV, Gu LC, Malefyt TR, Siahaan TJ. Methotrexate (MTX)-cIBR conjugate for targeting MTX to leukocytes: conjugate stability and *in vivo* efficacy in suppressing rheumatoid arthritis. J Pharm Sci. 2012; 101(9):3275–91. [PubMed: 22539217]
62. Manikwar P, Kiptoo P, Badawi AH, Buyuktimkin B, Siahaan TJ. Antigen-specific blocking of CD4-specific immunological synapse formation using BPI and current therapies for autoimmune diseases. Med Res Rev. 2012; 32(4):727–64. [PubMed: 21433035]
63. Badawi AH, Siahaan TJ. Immune modulating peptides for the treatment and suppression of multiple sclerosis. Clin Immunol. 2012; 144(2):127–38. [PubMed: 22722227]
64. The trials and tribulations of Tysabri. Lancet Neurol. 2006; 5(5):373. [PubMed: 16632299]
65. Sheridan C. Tysabri raises alarm bells on drug class. Nat Biotechnol. 2005; 23(4):397–8. [PubMed: 15815649]
66. Singer E. Tysabri withdrawal calls entire class into question. Nat Med. 2005; 11(4):359.
67. Sheridan C. Tysabri back on market. Nat Biotechnol. 2006; 24(8):874. [PubMed: 16900111]
68. Kobayashi N, Kobayashi H, Gu L, Malefyt T, Siahaan TJ. Antigen-specific suppression of experimental autoimmune encephalomyelitis by a novel bifunctional peptide inhibitor. J Pharmacol Exp Ther. 2007; 322(2):879–86. [PubMed: 17522343]
69. Kobayashi N, Kiptoo P, Kobayashi H, Ridwan R, Brocke S, Siahaan TJ. Prophylactic and therapeutic suppression of experimental autoimmune encephalomyelitis by a novel bifunctional peptide inhibitor. Clin Immunol. 2008; 129(1):69–79. [PubMed: 18676182]
70. Ridwan R, Kiptoo P, Kobayashi N, Weir S, Hughes M, Williams T, Soegianto R, Siahaan TJ. Antigen-specific suppression of experimental autoimmune encephalomyelitis by a novel bifunctional peptide inhibitor: structure optimization and pharmacokinetics. J Pharmacol Exp Ther. 2010; 332(3):1136–45. [PubMed: 20026673]
71. Brocke S, Gijbels K, Allegretta M, Ferber I, Piercy C, Blankenstein T, Martin R, Utz U, Karin N, Mitchell D, Veromaa T, Waisman A, Gaur A, Conlon P, Ling N, Fairchild PJ, Wraith DC, O'Garra A, Fathman CG, Steinman L. Treatment of experimental encephalomyelitis with a peptide analogue of myelin basic protein. Nature. 1996; 379(6563):343–6. [PubMed: 8552189]
72. Wraith DC. Autoantigenic peptide therapy in experimental autoimmune encephalomyelitis. Immunol Ser. 1993; 59:345–57. [PubMed: 7681697]
73. Buyuktimkin B, Kiptoo P, Siahaan TJ. Bifunctional Peptide Inhibitors Suppress Interleukin-6 Proliferation and Ameliorates Murine Collagen-Induced Arthritis. J Clin Cell Immunol. 2014; 5(6)
74. Murray JS, Oney S, Page JE, Kratochvil-Stava A, Hu Y, Makagiansar IT, Brown JC, Kobayashi N, Siahaan TJ. Suppression of type 1 diabetes in NOD mice by bifunctional peptide inhibitor: modulation of the immunological synapse formation. Chem Biol Drug Des. 2007; 70(3):227–36. [PubMed: 17718717]

75. McDevitt H. Specific antigen vaccination to treat autoimmune disease. Proc Natl Acad Sci U S A. 2004; 101(Suppl 2):14627–30. [PubMed: 15466699]
76. Metzler B, Burkhart C, Wraith DC. Phenotypic analysis of CTLA-4 and CD28 expression during transient peptide-induced T cell activation *in vivo*. Int Immunol. 1999; 11(5):667–75. [PubMed: 10330272]
77. Kim SK, Tarbell KV, Sanna M, Vadeboncoeur M, Warganich T, Lee M, Davis M, McDevitt HO. Prevention of type I diabetes transfer by glutamic acid decarboxylase 65 peptide 206–220-specific T cells. Proc Natl Acad Sci U S A. 2004; 101(39):14204–9. [PubMed: 15381770]
78. Herman AE, Tisch RM, Patel SD, Parry SL, Olson J, Noble JA, Cope AP, Cox B, Congia M, McDevitt HO. Determination of glutamic acid decarboxylase 65 peptides presented by the type I diabetes-associated HLA-DQ8 class II molecule identifies an immunogenic peptide motif. J Immunol. 1999; 163(11):6275–82. [PubMed: 10570321]
79. Tisch R, Wang B, Serreze DV. Induction of glutamic acid decarboxylase 65-specific Th2 cells and suppression of autoimmune diabetes at late stages of disease is epitope dependent. J Immunol. 1999; 163(3):1178–87. [PubMed: 10415012]
80. Buyuktimkin B, Wang Q, Kiptoo P, Stewart JM, Berkland C, Siahaan TJ. Vaccine-like controlled-release delivery of an immunomodulating peptide to treat experimental autoimmune encephalomyelitis. Mol Pharm. 2012; 9(4):979–85. [PubMed: 22375937]
81. Badawi AH, Kiptoo P, Siahaan TJ. Immune Tolerance Induction against Experimental Autoimmune Encephalomyelitis (EAE) Using A New PLP-B7AP Conjugate that Simultaneously Targets B7/CD28 Costimulatory Signal and TCR/MHC-II Signal. J Mult Scler (Foster City). 2015; 2(1)
82. Badawi AH, Kiptoo P, Wang WT, Choi IY, Lee P, Vines CM, Siahaan TJ. Suppression of EAE and prevention of blood-brain barrier breakdown after vaccination with novel bifunctional peptide inhibitor. Neuropharmacology. 2012; 62(4):1874–81. [PubMed: 22210333]
83. Badawi AH, Siahaan TJ. Suppression of MOG- and PLP-induced experimental autoimmune encephalomyelitis using a novel multivalent bifunctional peptide inhibitor. J Neuroimmunol. 2013; 263(1–2):20–7. [PubMed: 23911075]
84. Barenholz Y. Doxil(R)--the first FDA-approved nano-drug: lessons learned. J Control Release. 2012; 160(2):117–34. [PubMed: 22484195]
85. Perez AT, Domenech GH, Frankel C, Vogel CL. Pegylated liposomal doxorubicin (Doxil) for metastatic breast cancer: the Cancer Research Network, Inc. experience. Cancer Invest. 2002; 20(Suppl 2):22–9. [PubMed: 12442346]
86. Porche DJ. Liposomal doxorubicin (Doxil). J Assoc Nurses AIDS Care. 1996; 7(2):55–9.
87. Craig C. Current treatment approaches for neoplastic meningitis: nursing management of patients receiving intrathecal DepoCyt. Oncol Nurs Forum. 2000; 27(8):1225–30. quiz 1231–2. [PubMed: 11013903]
88. Chiechi LM. Estrasorb. IDrugs. 2004; 7(9):860–4. [PubMed: 15470604]
89. Beer JH, Springer KT, Coller BS. Immobilized Arg-Gly-Asp (RGD) peptides of varying lengths as structural probes of the platelet glycoprotein IIb/IIIa receptor. Blood. 1992; 79(1):117–28. [PubMed: 1728303]
90. Lieb E, Hacker M, Tessmar J, Kunz-Schughart LA, Fiedler J, Dahmen C, Hersel U, Kessler H, Schulz MB, Gopferich A. Mediating specific cell adhesion to low-adhesive diblock copolymers by instant modification with cyclic RGD peptides. Biomaterials. 2005; 26(15):2333–41. [PubMed: 15585236]
91. Schiffelers RM, Koning GA, ten Hagen TL, Fens MH, Schraa AJ, Janssen AP, Kok RJ, Molema G, Storm G. Anti-tumor efficacy of tumor vasculature-targeted liposomal doxorubicin. J Control Release. 2003; 91(1–2):115–22. [PubMed: 12932643]
92. Koning GA, Schiffelers RM, Wauben MH, Kok RJ, Mastrobattista E, Molema G, ten Hagen TL, Storm G. Targeting of angiogenic endothelial cells at sites of inflammation by dexamethasone phosphate-containing RGD peptide liposomes inhibits experimental arthritis. Arthritis Rheum. 2006; 54(4):1198–208. [PubMed: 16575845]
93. Wang Y, Wang L, Chen G, Gong S. Carboplatin-Complexed and cRGD-Conjugated Unimolecular Nanoparticles for Targeted Ovarian Cancer Therapy. Macromol Biosci. 2016

94. Fan R, Mei L, Gao X, Wang Y, Xiang M, Zheng Y, Tong A, Zhang X, Han B, Zhou L, Mi P, You C, Qian Z, Wei Y, Guo G. Self-Assembled Bifunctional Peptide as Effective Drug Delivery Vector with Powerful Antitumor Activity. Adv Sci (Weinh). 2017; 4(4):1600285. [PubMed: 28435772]

95. Khondee S, Baoum A, Siahaan TJ, Berkland C. Calcium condensed LABL-TAT complexes effectively target gene delivery to ICAM-1 expressing cells. Mol Pharm. 2011; 8(3):788–98. [PubMed: 21473630]

96. Chittasupho C, Xie SX, Baoum A, Yakovleva T, Siahaan TJ, Berkland CJ. ICAM-1 targeting of doxorubicin-loaded PLGA nanoparticles to lung epithelial cells. Eur J Pharm Sci. 2009; 37(2): 141–50. [PubMed: 19429421]

97. Muro S, Cui X, Gajewski C, Murciano JC, Muzykantov VR, Koval M. Slow intracellular trafficking of catalase nanoparticles targeted to ICAM-1 protects endothelial cells from oxidative stress. Am J Physiol Cell Physiol. 2003; 285(5):C1339–47. [PubMed: 12878488]

98. Muro S, Gajewski C, Koval M, Muzykantov VR. ICAM-1 recycling in endothelial cells: a novel pathway for sustained intracellular delivery and prolonged effects of drugs. Blood. 2005; 105(2): 650–8. [PubMed: 15367437]

99. Muro S, Mateescu M, Gajewski C, Robinson M, Muzykantov VR, Koval M. Control of intracellular trafficking of ICAM-1-targeted nanocarriers by endothelial Na+/H+ exchanger proteins. Am J Physiol Lung Cell Mol Physiol. 2006; 290(5):L809–17. [PubMed: 16299052]

100. Chittasupho C, Sestak J, Shannon L, Siahaan TJ, Vines CM, Berkland C. Hyaluronic acid graft polymers displaying peptide antigen modulate dendritic cell response *in vitro*. Mol Pharm. 2014; 11(1):367–73. [PubMed: 24283935]

101. Kuehl C, Thati S, Sullivan B, Sestak J, Thompson M, Siahaan T, Berkland C. Pulmonary Administration of Soluble Antigen Arrays is Superior to Antigen in Treatment of Experimental Autoimmune Encephalomyelitis. J Pharm Sci. 2017

102. Northrup L, Sestak JO, Sullivan BP, Thati S, Hartwell BL, Siahaan TJ, Vines CM, Berkland C. Co-delivery of autoantigen and b7 pathway modulators suppresses experimental autoimmune encephalomyelitis. AAPS J. 2014; 16(6):1204–13. [PubMed: 25297853]

103. Sestak J, Mullins M, Northrup L, Thati S, Forrest ML, Siahaan TJ, Berkland C. Single-step grafting of aminooxy-peptides to hyaluronan: a simple approach to multifunctional therapeutics for experimental autoimmune encephalomyelitis. J Control Release. 2013; 168(3):334–40. [PubMed: 23541930]

104. Sestak JO, Fakhari A, Badawi AH, Siahaan TJ, Berkland C. Structure, size, and solubility of antigen arrays determines efficacy in experimental autoimmune encephalomyelitis. AAPS J. 2014; 16(6):1185–93. [PubMed: 25193268]

105. Sestak JO, Sullivan BP, Thati S, Northrup L, Hartwell B, Antunez L, Forrest ML, Vines CM, Siahaan TJ, Berkland C. Codelivery of antigen and an immune cell adhesion inhibitor is necessary for efficacy of soluble antigen arrays in experimental autoimmune encephalomyelitis. Mol Ther Methods Clin Dev. 2014; 1:14008. [PubMed: 26015953]

106. Thati S, Kuehl C, Hartwell B, Sestak J, Siahaan T, Forrest ML, Berkland C. Routes of administration and dose optimization of soluble antigen arrays in mice with experimental autoimmune encephalomyelitis. J Pharm Sci. 2015; 104(2):714–21. [PubMed: 25447242]

107. Siliciano RF, Colello RM, Keegan AD, Dintzis RZ, Dintzis HM, Shin HS. Antigen valence determines the binding of nominal antigen to cytolytic T cell clones. J Exp Med. 1985; 162(2): 768–73. [PubMed: 2410534]

108. Siliciano RF, Keegan AD, Dintzis RZ, Dintzis HM, Shin HS. The interaction of nominal antigen with T cell antigen receptors. I. Specific binding of multivalent nominal antigen to cytolytic T cell clones. J Immunol. 1985; 135(2):906–14. [PubMed: 2409158]

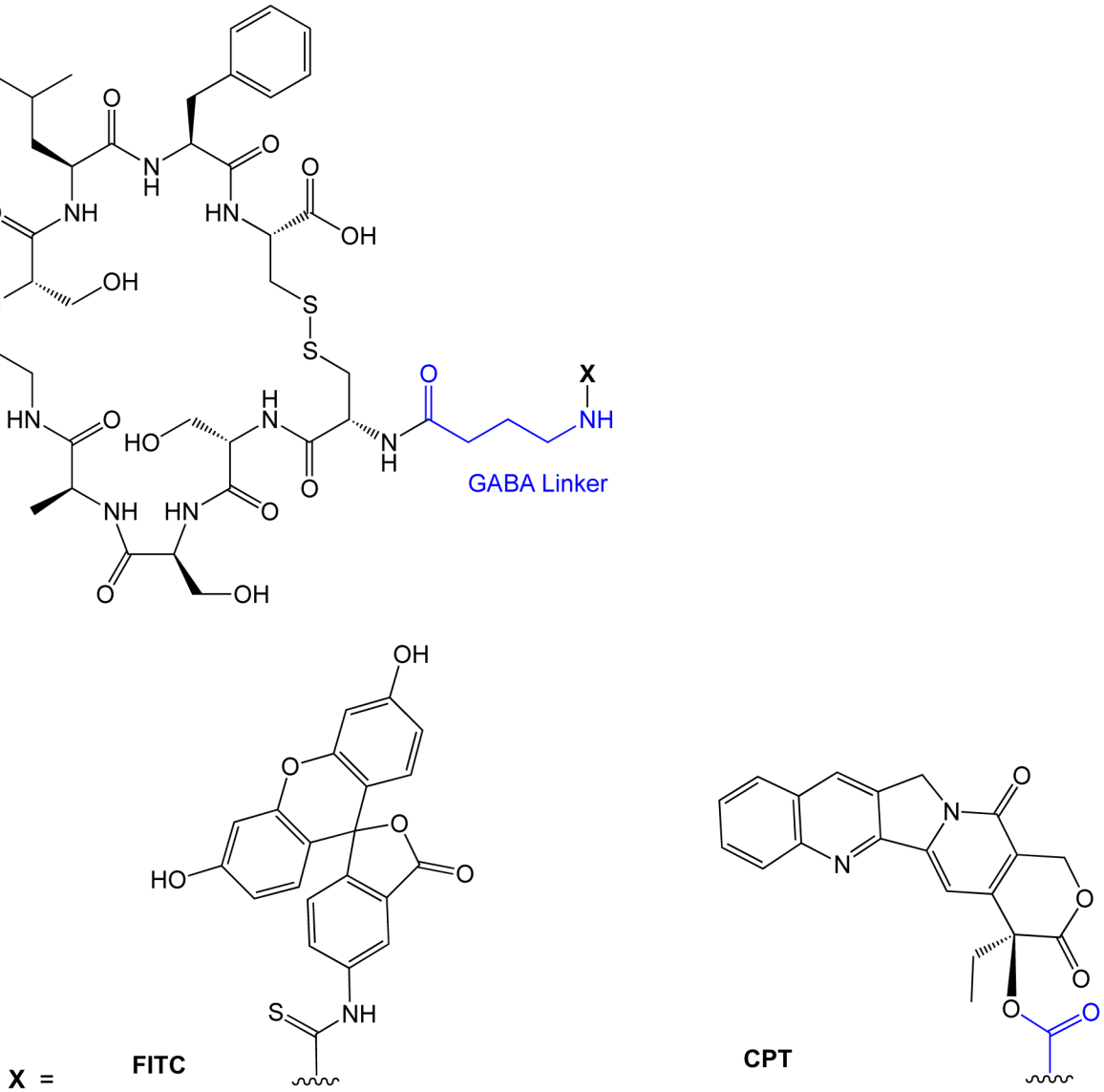

Figure 1.

ALOS4 Conjugates. ALOS4 peptide conjugated with either FITC or camptothecin using a GABA linker.

Figure 2(A).

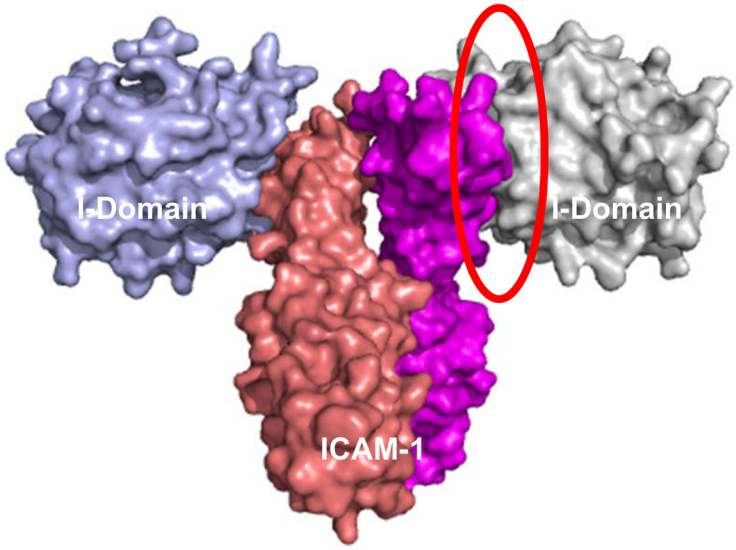

PDB ID: 1MQ8

Figure 2(B).

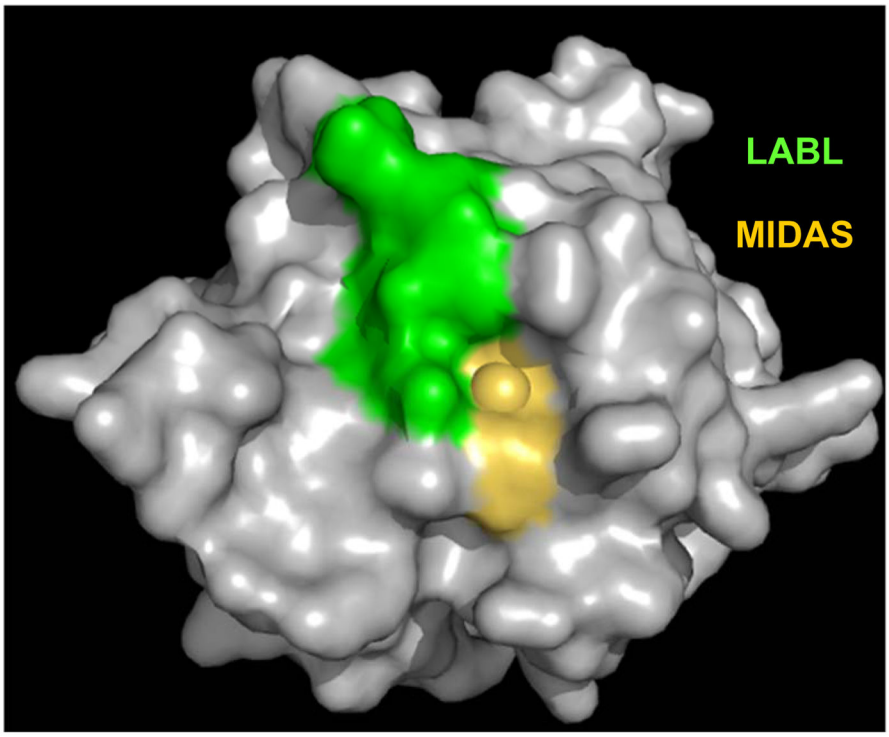

Figure 2(C).

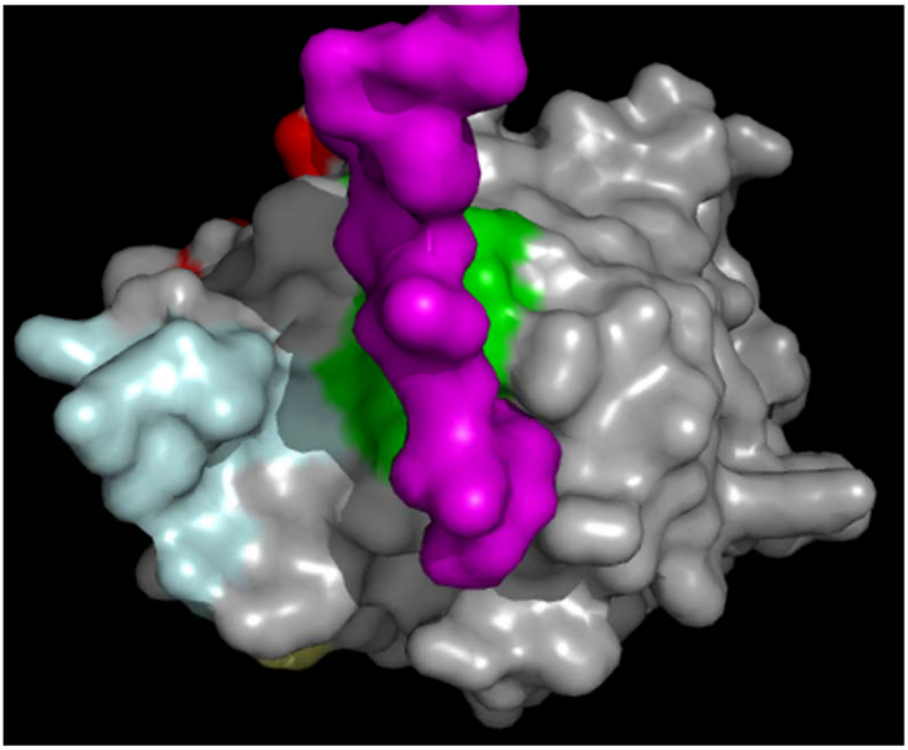

Figure 2(D).

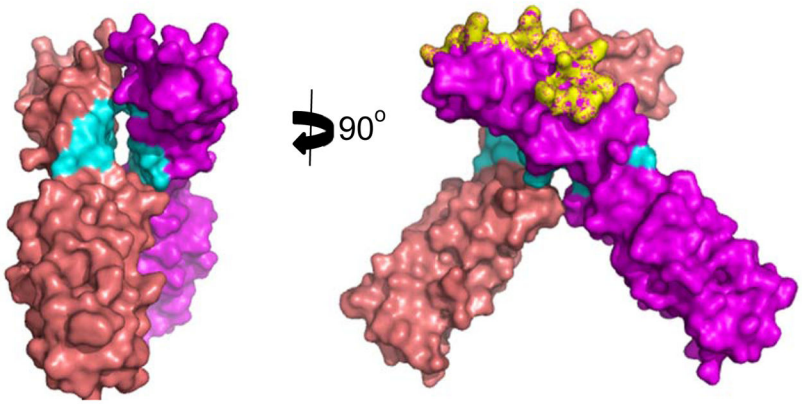

Figure 2.

X-ray structure of LFA-1 I-Domain in complex with ICAM-1 (PDB: 1MQ8). (A) ICAM-1 protein forms a homodimer, which interacts with two separate I-domains of LFA-1 at each D-1 domain of ICAM-1. Counter-clockwise quarter-turn on the encircled interface shows (B) the interacting region of LFA-1 I-domain with ICAM-1, also referred to as the MIDAS region (yellow/gold), which overlaps with the region of the LABL peptide sequence (green). (C) Shows the region on LFA-1 interacting with the IEL sequence (purple) from ICAM-1.

(D) Maps regions on the ICAM-1 homodimer where IB (cyan) and IE (yellow) peptide sequences are located.

Figure 3(A) i-iii.

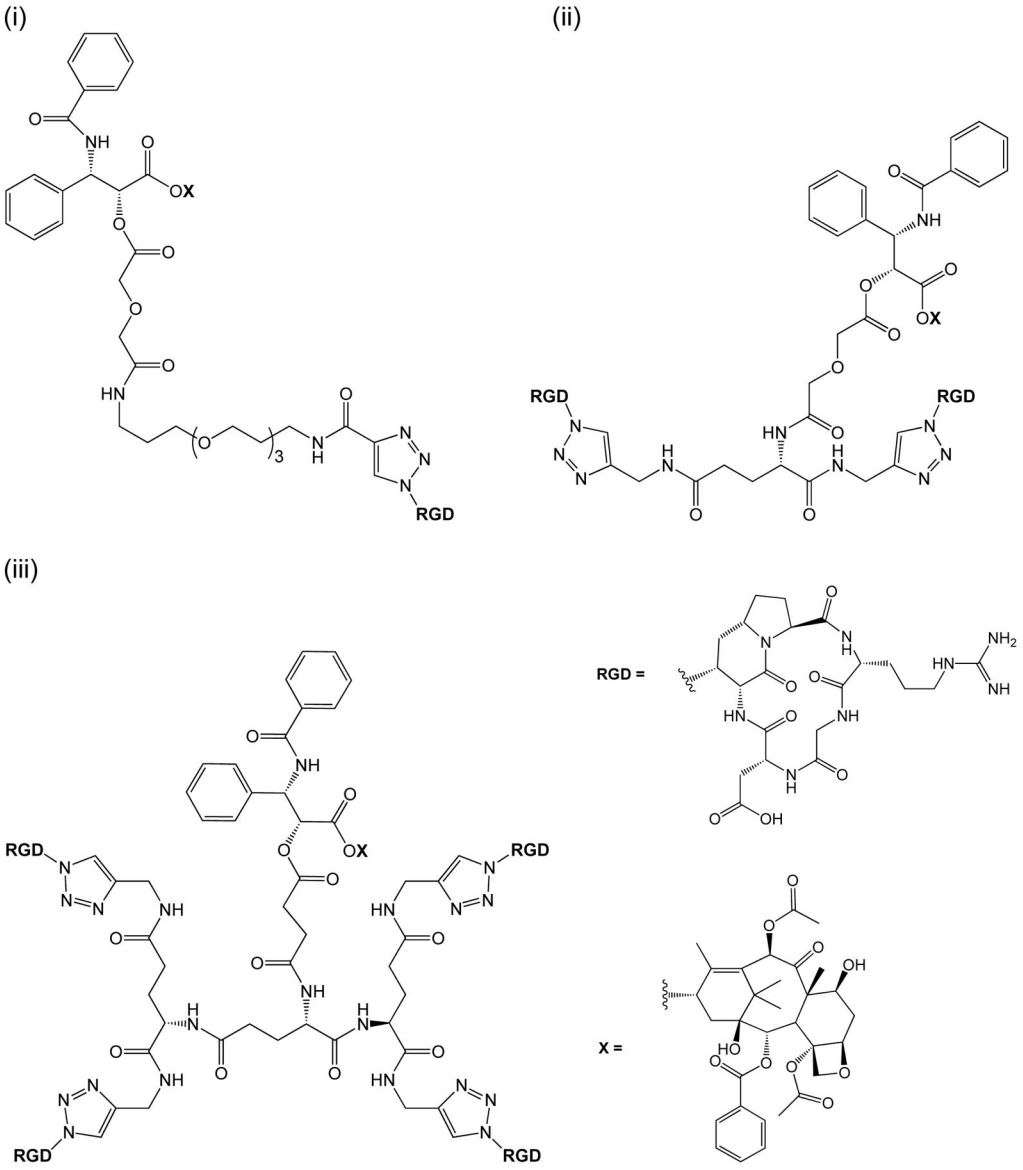

Figure 3(B).

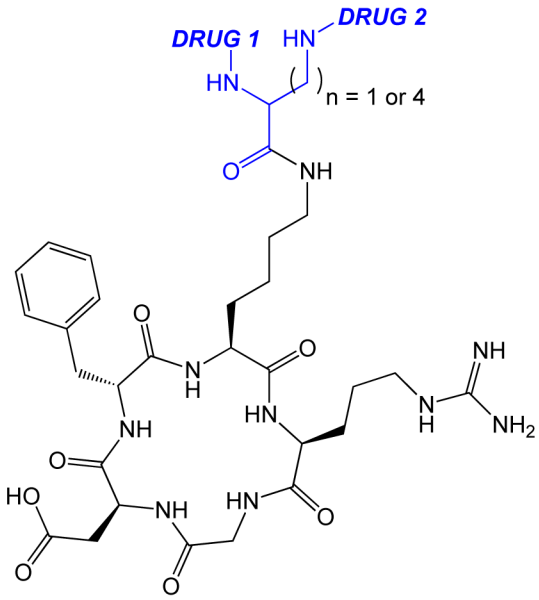

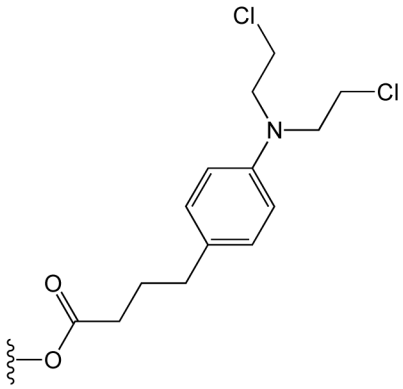

CLB

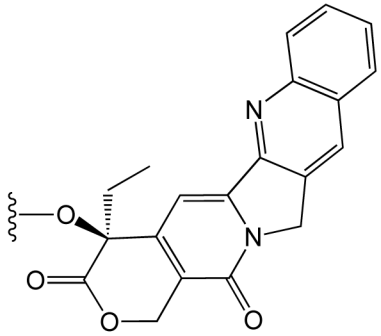

CPT

Figure 3(C) i-ii.

(i)

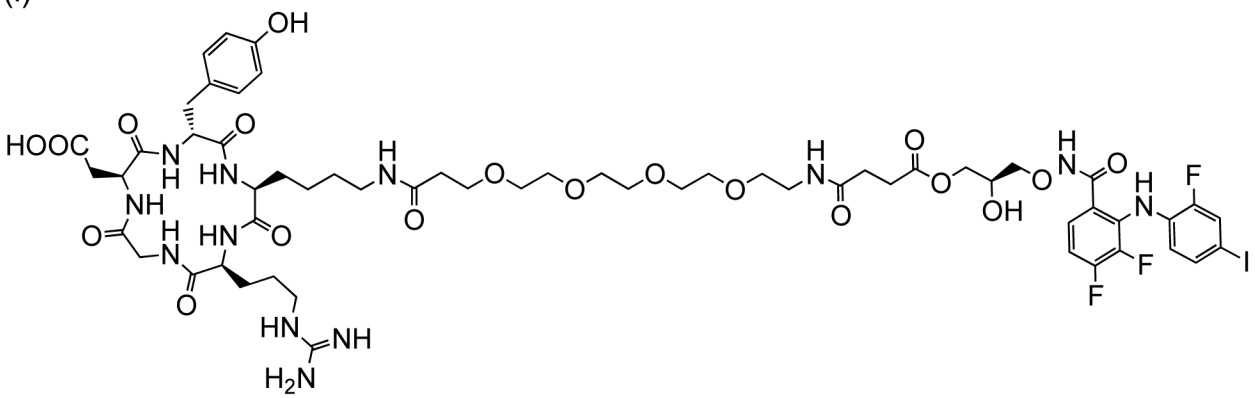

(ii)

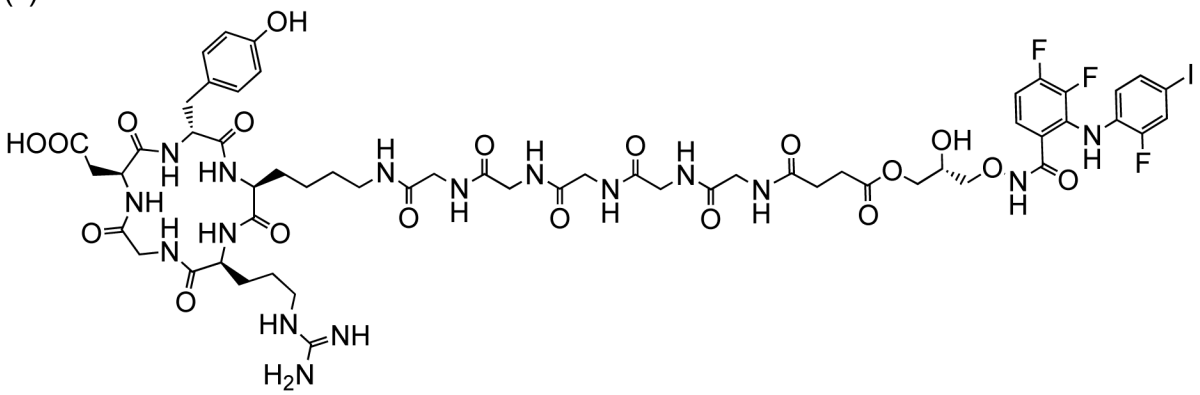

Figure 3(D).

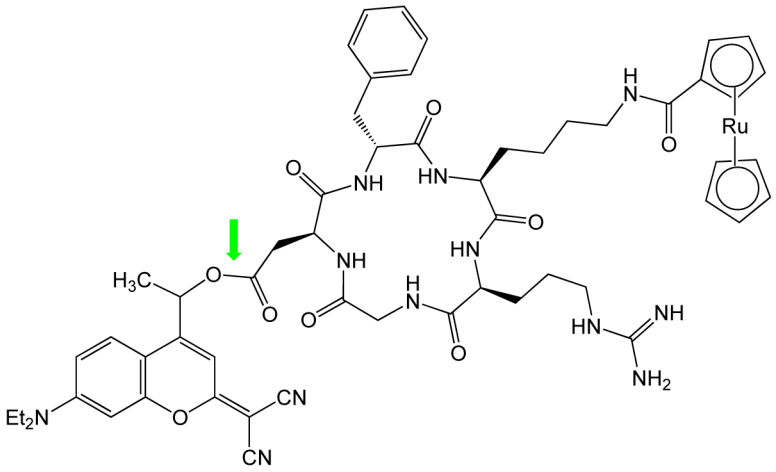

Figure 3(E).

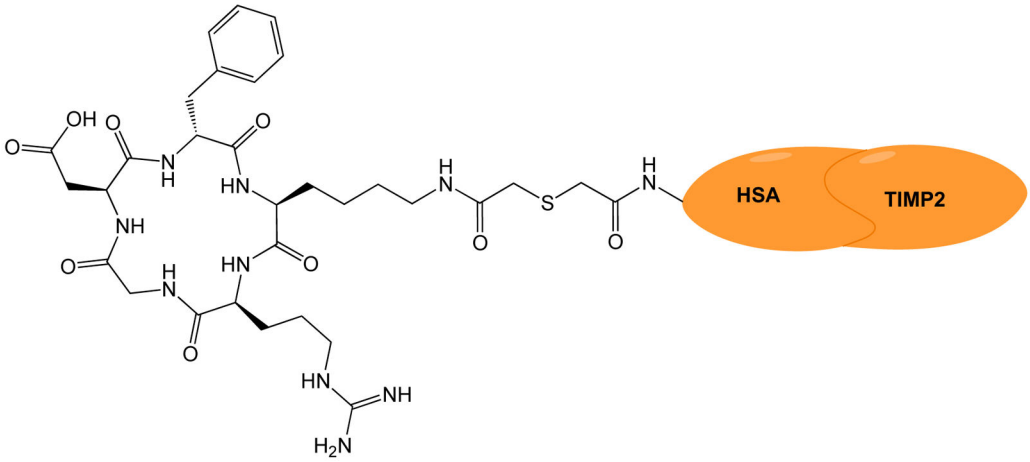

Figure 3.

RGD peptide drug conjugates. (A) RGD-PTX conjugates bearing: (i) monovalent, (ii) bivalent, and (iii) tetravalent RGD units; (B) Dual-Drug-RGD conjugates with camptothecin and/or chlorambucil; (C) W22-RGD conjugates using (i) PEG and (ii) amide linkers; (D) Photocontrolled RGD conjugate bearing a cleavable bond (green arrow) with a “caging” DEAdcCE group; and (E) RGD-HSA-TIMP2 conjugate, where cyclic RGDfK is linked to a fusion protein (HSA/TIMP2) through a thioether bond.

Figure 4(A-B).

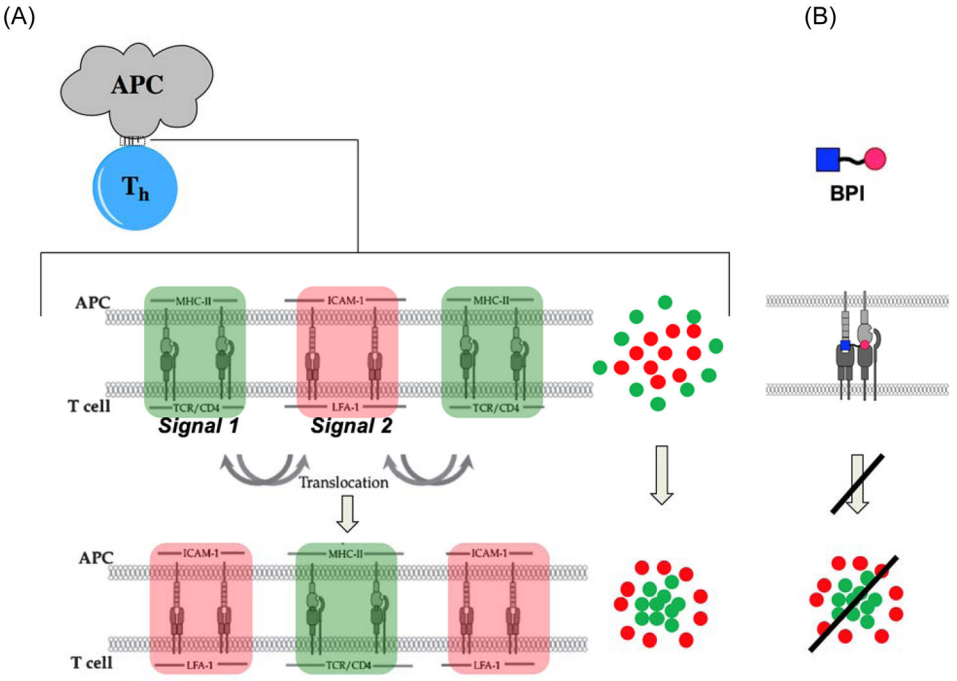

Manikwar, P., et al.., Medicinal Research Reviews. 32, No. 4, 727--764, 2012

Figure 4.

Inhibition of intercellular Signal-1/Signal-2 surface protein interactions between antigen-presenting (APC) and docked T-helper (T_h) cells. Intercellular protein complexes cluster and translocate (A) to form the immunological synapse (IS), which precludes the triggering of inflammatory response processes. (B) Bifunctional peptide inhibitors (BPI), comprised of a covalently linked antigenic and Signal-2 inhibitor peptide (LABL), mimic interacting surfaces of both Signal-1 and -2 complexes, and preclude inflammatory responses by disrupting the protein clustering and translocation required in the IS, presumably due to the non-cleavable peptide linker.

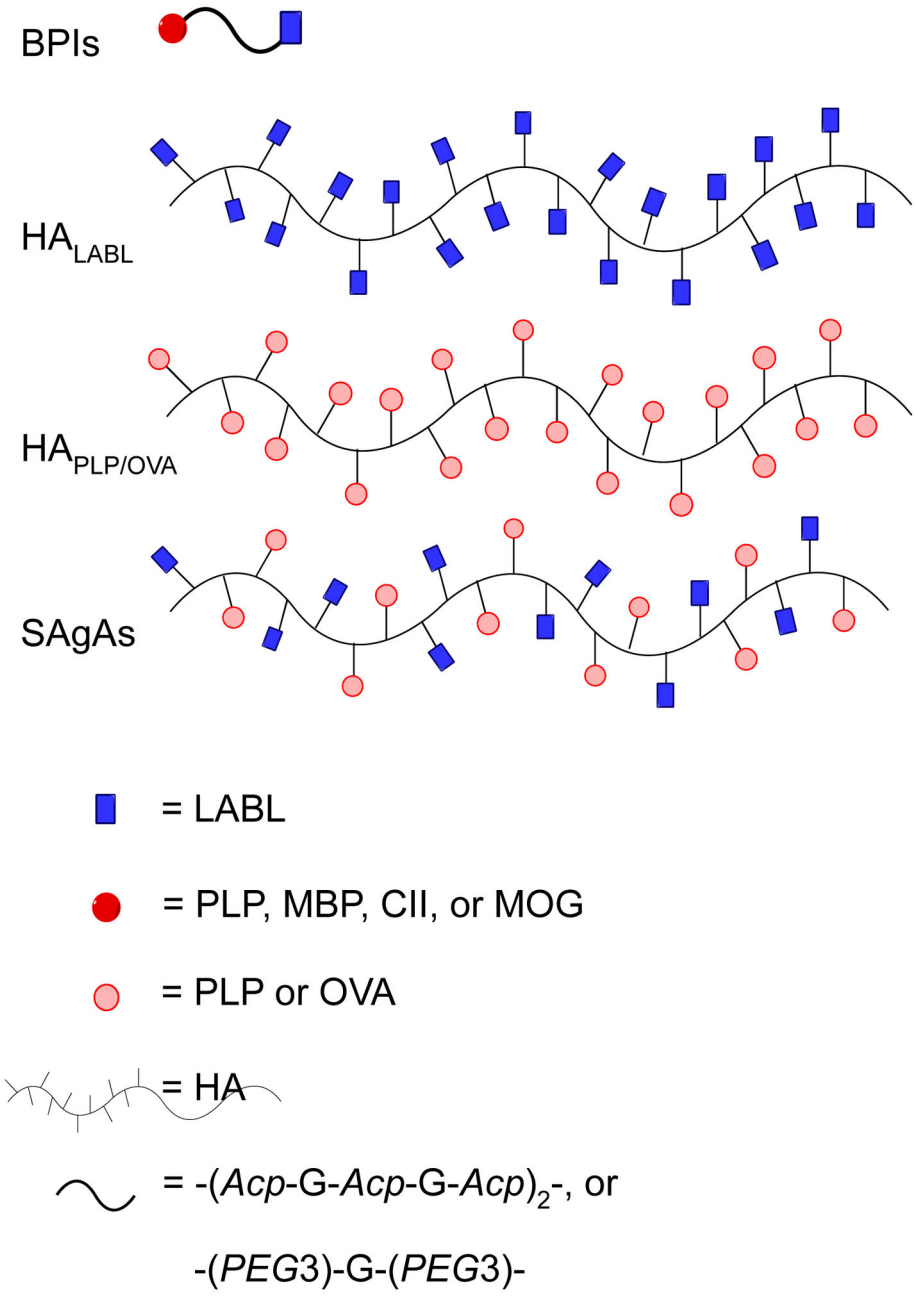

Figure 5.
Derivatized hyaluronic acid (HA) polymers with multiple units of either conjugated antigenic or Signal-2 inhibiting peptides. Analogous to BPIs are Soluble Antigen Arrays (SAgAs), which are similarly derivatized HA polymers with multiple units of both antigenic and Signal-2 inhibitor peptides. Figure 1.

Table 1

Peptide Names and Sequences

Name	Peptide Sequence
RGD in Cilengitide	Cyclo(RGDfK)
RGD	Cyclo(RGDfV)
RGD	Cyclo(RGDyV)
RGD in W22 PDC	Cyclo(RGDyK)
RGD in PAMAM	Cyclo(RGDfC)
$3PRGD_2$	PEG_4-E[PEG_4-c(RGDfK)]$_2$
ALOS-4	Cyclo1,9(CSSAGSLFC)
IB	QTSVSPSKVILPRGGSVLVTC
cIBR	Cyclo1,12(PenPRGGSVLVTGC)
IE	DQPKLLGIETPLPKKELLLPGNNRK
cIEL	Cyclo1,12(PenDQPKLLGIETC)
LABL	ITDGEATDSG
cLABL	Cyclo1,12(PenITDGEATDSGC)
PLP	HSLGKWLGHPDKF
PLP-BPI	Ac-HSLGKWLGHPDKF-(AcpGAcpGAcp)$_2$-ITDGEATDSG-NH_2
MOG	GWYRSPFSRVVHL
MOG-BPI	Ac-GWYRSPFSRVVHL-(PEG_3)-G-(PEG_3)-ITDGEATDSG-NH_2
PLP-MOG-BPI	Ac-GWYRSPFSRVVHL -(PEG_3)-G-(PEG_3)-ITDGEATDSG-(PEG_3)-G-(PEG_3)-HSLGKWLGHPDKF-NH_2
MBP	ASQKRPSQRSK
MOG	GWYRSPFSRVVHL
OVA	AVHAAHAEINEA
CII-1	PPGANGNPGPAGPPG
CII-2	Ac-GEPGIAGFKGEQGPK-NH_2
CII-3	Ac-QYMRADEADSTLR-NH_2
CII-BPI-1	Ac-PPGANGNPGPAGPPG-(AcpGAcpGAcp)$_2$-ITDGEATDSG-NH_2
CII-BPI-2	Ac-GEPGIAGFKGEQGPK-(AcpGAcpGAcp)$_2$-ITDGEATDSG-NH_2
CII-BPI-3	Ac-QYMRADEADSTLR-(AcpGAcpGAcp)$_2$-ITDGEATDSG-NH_2
HRK-19	HAVRNGRRGDGGAVPIAQK
TAT	RKKRRQRRR
TAT-PEG-LABL	RKKRRQRRR-(Peg)$_n$-ITDGEATDSG
GAD	EIAPVFVLLE
GAD-BPI	EIAPVFVLLE-(AcpGAcpGAcp)-ITDGEATDSG